UNITED NATIONS UNIVERSITY
GEOTHERMAL TRAINING PROGRAMME
Orkustofnun, Grensásvegur 9,
IS-108 Reykjavík, Iceland

Reports 2009
Number 9

INTERPRETATION OF RESISTIVITY SOUNDINGS IN THE KRÝSUVÍK HIGH-TEMPERATURE GEOTHERMAL AREA, SW-ICELAND, USING JOINT INVERSION OF TEM AND MT DATA

Sudian A. Chiragwile
Geological Survey of Tanzania (GST)
P. O. Box 903
Dodoma,
TANZANIA
sudichi@yahoo.com

ABSTRACT

The resistivity structure of the Krýsuvík high-temperature geothermal field, SW-Iceland, has been outlined by using a joint inversion of Transient Electromagnetic (TEM) and Magnetotelluric (MT) data. The TEM method delineates resistivity structures at a depth ranging from tens of metres down to almost 1,000 m whereas MT signals delineate resistivity structures down to a depth of several tens of kilometres. Joint inversion of TEM and MT data is useful in correcting for the static shift of MT data, which can cause large errors in the interpretation. Both the TEM and MT data reveal a low-resistivity cone shaped zone. The low resistivity is closest to the surface in the fracture zone. Below the conductive zone, there is a resistive core.

The MT and TEM electrical methods resolve resistivity layers with the resistivity differences mainly based on alteration. The layers consist of different clay minerals e.g. smectite and zeolite, mixed-layer clay, chlorite and epidote. The zone where the smectite-zeolite clay minerals are dominant is located above the mixed-layer clay zone. The chlorite-epidote zone is located below it and formed at higher temperatures than the clay minerals above. The top layers presumably consist of unaltered volcanic lava flows while the bottom part consists of a core body with resistive high-temperature minerals and intrusive dykes.

The geothermal field in the Krýsuvík area is associated with faults that form a shallow graben demarcated by the major fault lineaments. The two fault lineaments might be responsible for recharging or discharging water back and forth from the deep heat source. The dyke swarm may connect to a deep magmatic chamber. The electrically conductive zone relates to the faults. High-temperature geothermal fluid has caused the hydrothermal alteration of the rocks and formed clay minerals that occur in zones dependent on temperature. The interpretation of TEM and MT data shows that development of the geothermal resource is confined to two major lineaments. The electrically conductive zone and the associated resistive core lie between the two lineaments. Similar structures are at a greater depth outside the lineaments. Thus, the interpretation of the electrical resistivity data suggests that the drill holes planned for mining the high-temperature reservoir should be localised within the shallow graben. The holes should be drilled through the conductive layer and well into the highly resistive core.

1. INTRODUCTION

TEM and MT methods are used extensively in the exploration of geothermal resources because of their advantages in investigating deep subsurface features. The TEM and MT equipment need little space, a small work force and are applicable in difficult terrain. Hersir and Björnsson (1991) describe the application of electrical resistivity methods in the exploration of geothermal resources in Iceland that began in the 1950s. Direct current methods, such as Schlumberger vertical soundings, the dipole-dipole method and head-on profiling were used up to the early 1990s. They have now been replaced by the transient electromagnetic (TEM) and magnetotelluric (MT) methods.

The electrical resistivity structures in the Krýsuvík high-temperature geothermal field were analysed through a profile with soundings based on the TEM and MT methods. The profile lies in a NW-SE direction, perpendicular to the major geological structures that trend at about N40°E. The measured TEM and MT data (raw data) were processed and modelled for estimating the electrical resistivity structure of the subsurface. Raw data from the TEM instruments were processed using the TEMX program. The signal to noise ratio in MT signatures was maximised by using synchronised data from a remote reference MT-station. Before further analyses, outlier points were removed manually. The synchronized remote and local MT data were used to remove uncorrelated cultural noise between the two MT-stations.

After being processed at an initial stage to increase the signal to noise ratio, the TEM and MT data sets were interpreted by using forward (numerical modelling) or inversion modelling techniques (Occam). A joint inversion of TEM and MT was used to fit the observed and calculated curves in order to estimate the subsurface resistivity structure and infer a geological structure that relates to the geothermal system. Results of the joint inversion modelling of the TEM and MT data were integrated with geological and geochemical data obtained from a drill hole to better understand the resistivity structures.

The reason for conducting a joint inversion of the MT and TEM data is that the apparent resistivity of MT soundings tends to shift due to the presence of near-surface inhomogeneities. This static shift can mislead the interpretation. On the other hand, TEM signatures do not experience a static shift since they only measure the magnetic field, not the electric field. Therefore, TEM data were used to correct the static shift of the MT data, with the MT-curve tied in. The joint inversion program uses MT and TEM data sets from sites located very close to each other to correct the shift by inverting the two data sets simultaneously until the MT and TEM data sets both fit reasonably well; one of its outcomes is a shifting factor. Sternberg et al. (1988) have shown that TEM data from a site separated from the MT site by a distance in the range of 0-100 m, or where the MT site is within the TEM loop, can be used for static shift corrections.

The main objective of conducting the electrical resistivity survey in the Krýsuvík area was to delineate the resistivity structure for the development of the geothermal resource in the area. One of the challenges encountered in many exploration surveys for high- and low-temperature geothermal resources is to locate the reservoirs or the heat source of geothermal fluids. Geothermal fields are explored by the integration of various methods, such as geological mapping (structures and lithology), geochemical analyses of geochemical fluids, mapping of mineral alteration, geophysical exploration methods and drilling and analysis of thermal gradients. At early stages, most methods use data from surface manifestations except geophysical methods that aim at locating and describing subsurface structures that relate to geothermal potentials in the area. In addition to the ability of geophysical methods to delineate subsurface structures, the methods are cost effective compared to drilling costs. Cost effectiveness and risk minimization make geophysical surveys a vital technique prior to a drilling programme in the development of geothermal resources. Detailed geophysical exploration resolves geophysical anomalies and narrows down the targets. Various geophysical methods are used for geothermal exploration purposes. The most popular and useful methods in estimating the depth to the reservoirs, and locating the drilling targets in Iceland are electrical resistivity methods. Hersir and

Björnsson (1991) classify geophysical methods in geothermal exploration as direct and structural methods. Direct methods include electrical and thermal methods.

Direct methods are based on physical parameters that relate directly to the presence of hot water or geothermal fluids. Structural methods, including gravity, magnetic and seismic methods, are used to delineate geological structures such as intrusive bodies or tectonic lineaments that might control the flow of the fluid.

In the Krýsuvík area, the conceptual model of the geothermal field is based on geophysical data; geochemical data and the geological features observed on the surface. The clear matching results support the application of the electrical resistivity method in exploring geothermal resources. Conceptual models of geothermal fields may vary from one region to another. In Iceland, basaltic clay mineral alteration in the active volcanic zone is also characteristic for the Mid-Atlantic oceanic ridge. The common geological models of mid-oceanic ridges are typically extensional fault systems intruded by basalts in the form of dykes, and surface basalt lavas on eruptive fissures. The fault system may form a graben/basin, and the erupted material a ridge parallel to the faulting lines. Major faults may be connected to deep zones of high-temperature bodies. Then, these fractures tap heat from the crust by the injection of cold water and the discharge of hot water to form geothermal reservoirs.

In volcanic regions, especially within the mid-oceanic-ridges, basaltic rocks are composed of common primary minerals. Basalts in the Mid-Atlantic ridge are mainly tholeiitic, composed of pyroxene, olivine and calcium rich plagioclase (anorthite). The hydrothermal alteration of the primary minerals depends on the temperature distribution. The temperature distribution is determined by heat convection (hydrothermal waters) that causes mineral alteration in the volcanic regime and forms various clay minerals. These clay minerals have varying electrical conductivity properties, thus becoming a significant factor in the search for the geothermal heat source. Figure 1 shows the zonal distribution of clay minerals with depth. The zone dominated by smectite-zeolite minerals has a low electrical resistivity (high conductivity) while the chlorite-epidote zone has high electrical resistivity (low conductivity). The differences in these clay mineral characteristics are an important reason for resistivity methods being used in the exploration of geothermal resources.

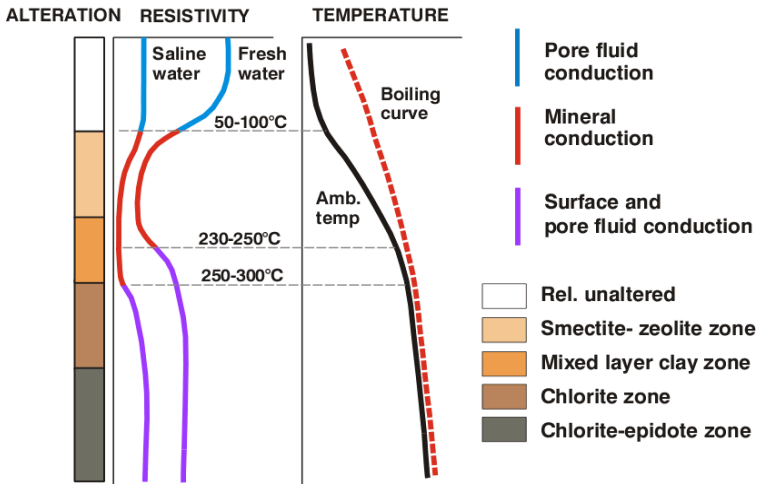

FIGURE 1: Electrical conduction vs. temperature and hydrothermal alteration (Flóvenz et al., 2005)

Economically exploitable geothermal resources are located at depth from a few hundred metres to a few kilometres. Some electrical methods have a good depth of penetration, which is necessary for resolving the resistivity structures of the subsurface features. The effective methods for investigations at depths include electromagnetic (TEM and MT) and direct current (DC) methods like the Schlumberger and the dipole-dipole layouts. The DC methods are less penetrative than the TEM and in particular MT. Their depth penetration depends on the distance between the current and potential electrodes. Another factor that affects the DC methods is that due to near-surface inhomogeneities, these methods suffer the same static shift problem as MT soundings (Hersir and Björnsson, 1991). The induction transient electromagnetic (TEM) method has a similar depth of penetration as DC methods. The depth of investigation using TEM is in the range of a few tens of metres to a kilometre, depending on the configuration setup and the instruments used. The depth of investigation using the

MT method ranges from a few metres to tens or even hundreds of kilometres depending on the instruments used and the recording time. Generally, induction coil magnetometers can respond well to magnetic fluctuations with periods between 0,001 to 3,600 s whereas fluxgate magnetometers cover periods between 10 to 100,000 s (Simpson and Bahr, 2005).

Technical advantages that favour electromagnetic methods (TEM and MT) for penetrating to a great depth include the utilisation of induced or secondary signals from the subsurface in the interpretation of subsurface electrical structures and their characteristics. The induction principle relates primary electromagnetic fields that induce secondary electromagnetic fields in the subsurface. The responses of the subsurface structures depend on their electromagnetic physical characteristics. Recursive relationships infer the vertical variations of the layers according to their electrical properties (Árnason, 1989; Gubbins, 2004; Simpson and Bahr, 2005).

2. LITERATURE REVIEW

The literature review summarises the fundamental principles of electromagnetic waves, induction processes and rock properties. In addition, this part introduces the resistivity of rocks and the parameters that cause variations in the resistivity of rocks and the effects caused by high-temperature geothermal water. Finally, it shows the relationship between high-temperature geothermal fields and resistivity and the application of electrical methods in the exploration of geothermal resources.

2.1 Propagation of electromagnetic waves

Electromagnetic methods in geophysics have been developed since the 1950s by Cagniard (1953) and Tikhonov (1950), based on Maxwell's equations that are composed of Ampère's, Gauss's and Faraday's law (Equations 1-7) as expressed by Jones et al. (1989), Vozoff (1991) and Zhdanov and Keller (1994). The equations describe the magnetic and electric fields and their relationship. The strength of the electromagnetic fields varies from one body to another depending on the petrophysical properties of the body and other factors. The essential physical properties of electromagnetic fields are electrical resistivity or conductivity, magnetic permeability and electric permittivity. The physical properties link the electromagnetic induction to the transmission and the receiver. The counteraction of electric and magnetic fields causes electromagnetic fields to travel, and diffuse from the air to the subsurface. The physical properties of rocks govern the propagation and the depth of penetration of the electromagnetic waves in the subsurface. The electromagnetic induction processes require a primary wave source (transmitter) and a conductor.

Faraday's Law: $$\boldsymbol{\nabla x E} = -\mu \frac{\partial \boldsymbol{H}}{\partial t} \quad (1)$$

Ampère's Law: $$\boldsymbol{\nabla x H} = \boldsymbol{j_c} + \frac{\partial \boldsymbol{D}}{\partial t} \quad (2)$$

Coulomb's Law: $$\boldsymbol{\nabla \cdot D} = Q \quad (3)$$

Gauss's Law: $$\boldsymbol{\nabla \cdot B} = 0 \quad (4)$$

Ohm's Law: $$\boldsymbol{J} = \sigma \boldsymbol{E} \quad (5)$$

$$\boldsymbol{B} = \mu \boldsymbol{H} \quad (6)$$

$$\boldsymbol{D} = \varepsilon \boldsymbol{E} \quad (7)$$

Electrical exploration techniques describe the subsurface structures based on the contrasts of their resistivity or conductivity. An electrical field crossing a subsurface boundary of different electrical resistivities produces a potential difference. The presence of a potential difference and resistivity generates an electrical current in the subsurface; this, in turn, generates another magnetic field. In that way, electrical and magnetic fields continue to diffuse vertically downwards. Telford et al. (1990) outlined different models of electromagnetic bodies in the subsurface including homogeneous half space models, spherical bodies located near the surface and layered models located from shallow to great depths. The half space model defines the subsurface as the conductor while the transmitter (source of waves) and the receiver are located in the half space.

Electromagnetic wave propagations in subsurface bodies or layers generate secondary signals based on the existing physical properties. The responses from the conductors (secondary signals) compared to the primary (transmitted) signal are used to characterise the subsurface bodies. The depth to the structure of interest is estimated, based on the period or frequency of the transmitted signals and the frequency of the secondary signals. Árnason (1989) shows how primary and secondary signals characterise or resolve the properties of the subsurface (conductor); the depth of penetration/diffusion of signals from the transmitter to the conductor is found by first characterising the uppermost layer, which is then used as an initial model to estimate the characteristics of successive layers.

The aforementioned fundamental Maxwell´s equations describe the electromagnetic fields in a source free region. Time varying magnetic fields generate electrical currents (conduction and displacement currents) while time varying electric fields induce magnetic fields in the conductor. The combination of Equations 1-7 gives the expression of the telegrapher's equations for wave propagation in a homogeneous medium as shown in Zhdanov and Keller (1994).

$$\nabla x \nabla x H = \nabla x \left(\sigma \mu H + \varepsilon \mu \frac{\partial}{\partial t} H \right) = \sigma \mu \frac{\partial H}{\partial t} + \varepsilon \mu \frac{\partial^2 H}{\partial t^2} \tag{8}$$

$$\nabla x \nabla x E = \nabla x \left(\sigma \mu E + \varepsilon \mu \frac{\partial}{\partial t} E \right) = \sigma \mu \frac{\partial E}{\partial t} + \varepsilon \mu \frac{\partial^2 E}{\partial t^2} \tag{9}$$

$$\nabla^2 (E, H) - \sigma \mu \frac{\partial (E, H)}{\partial t} - \varepsilon \mu \frac{\partial^2 (E, H)}{\partial t^2} = 0 \tag{10}$$

Plane wave Equation 2c can be rewritten and simplified; see Equation 3. The wave equation shows the dependency between the magnetic and electric fields. Later it will be shown that constant k, defined as the propagation constant, includes the physical properties of the subsurface structures (refer to Equations 23 -27).

$$\nabla^2 \boldsymbol{E} + k^2 \boldsymbol{E} = 0 \tag{11}$$

$$\nabla^2 \boldsymbol{H} + k^2 \boldsymbol{H} = 0 \tag{12}$$

One of the concerns in the exploration of geothermal, hydrocarbons, and other natural resources, such as mineral deposits, is the estimation of the depth of investigation. The depth of investigation depends on the selected method, and the physical properties of the structures being investigated. The penetration depths of electromagnetic waves depend on various parameters: the geometric configuration of the instruments, the strength of the primary signal and the earth/subsurface response, the number of windings and the cross-sectional area of the coils, the distance between the transmission and receiving loops, the current or magnetic moments in the coil, the transmitted frequencies, and sampling time. Use of long sampling periods or low frequencies enables deeper subsurface investigations.

On the other hand, the propagation constant (k) and the response of layered earth depends on its petrophysical properties such as conductivity (σ) or resistivity (ρ), magnetic permeability (μ), electrical permittivity (ε) and the transfer functions of the electromagnetic waves in the subsurface. Telegrapher's equation (Equation 10) suggests that subsurface materials behave as conductors, insulator/non-conductive or semi-conductors. Therefore, it is assumed that the subsurface of the Earth varies with conductivity, and dielectric and magnetic permeability. In some cases, there are great contrasts in the physical properties so that the electromagnetic waves behave as quasi-stationary (quasi-static) or as a diffusion wave. The propagation constant k in Equations 11 and 12 is significant because it relates to the electrical and magnetic properties in the TEM and MT methods. The boundaries of the layers are characterised by large contrasts in physical properties. The contrasts in conductivity reflect, in particular, in the electric field while the magnetic field may show insignificant changes. At the boundary, an accumulation of electrical charges generates an electric field that opposes the induced electric field.

As the electromagnetic waves propagate into the subsurface, the amplitudes or the strength of the waves diminish with depth. Vozoff (1991) argues that electromagnetic waves decay due to attenuation effects. Electromagnetic waves attenuate with depth logarithmically or exponentially as they propagate downwards into the subsurface. The depth of penetration depends on:

- Amplitude of the initial signal at the surface ($\boldsymbol{E_0}$, $\boldsymbol{H_0}$),
- Sinusoidal time variation ($\boldsymbol{E}$, $\boldsymbol{H}$)$e^{i\omega t}$,
- Sinusoidal depth variation ($\boldsymbol{E}$, $\boldsymbol{H}$)$e^{-i\alpha z}$, and
- Exponential decay with depth ($\boldsymbol{E}$, $\boldsymbol{H}$)$e^{-\alpha z}$

These attenuation and decay properties combine and give the wave propagation, as seen in Equations 13 and 14:

$$(\boldsymbol{E}) = (\boldsymbol{E}_0)e^{i\omega t}e^{-i\alpha z}e^{-\alpha z} \tag{13}$$

$$(\boldsymbol{H}) = (\boldsymbol{H}_0)e^{i\omega t}e^{-i\alpha z}e^{-\alpha z} \tag{14}$$

2.2 Electrical resistivity of rocks

Varying temperatures and pressure can cause changes in the electrical resistivity of rocks. Temperature and pressure depend on depth, tectonic activity and anomalous magmatic heat sources. The change in temperature and pressure causes changes in the physical properties of the rocks due to changes in chemical reactions and other physical parameters. For example, the secondary mineralisation that fills pore spaces may reduce porosity; the dissolution of some minerals may increase porosity. Density may increase with depth in sedimentary rocks due to compaction and a reduction of pore spaces caused by pressure. One significant chemical change that relates resistivity and geothermal fields is mineral alteration.

Mineral alteration is a chemical reaction that depends on mineral content, pressure defined by depth and temperatures of the hydrothermal fluid. Hydrothermal fluids may vary in salinity or pH and that may accelerate mineral alteration.

The resistivity of water-saturated rocks depends on many physical parameters such as porosity, salinity of the saturated fluid, temperature, and conductivity of the rock matrix. A useful and simplified formula approximates the resistivity of rocks/formations, referred to as Archie's law and shown in Equation 15:

$$\rho = \rho_w a \emptyset^{-m} \tag{15}$$

where ρ = Bulk (measured) resistivity;

ρ_w = Resistivity of the pore fluid;
$\emptyset$ = Porosity in proportions of total volume of the formation or rocks;
a and m = Empirical parameter (around 1) and cementing factor (around 2), respectively.

Rocks are composed of rock forming minerals such as metals, sulphides, oxides, silicates, carbonates, tellurides and arsenides embedded in matrices. The minerals and matrices respond differently to electromagnetic waves. Water content in rocks is one of the main characteristics in geothermal fields. Water content depends on the texture (crystalline, porosity, fractures, interconnection between pores, or the presence of fossil water enclosed in pores). On a micro-scale, rock-forming minerals are composed of crystal lattices that carry the mineral properties or chemical properties, physical and electrical properties (e.g. conductivity and magnetic properties such as susceptibility or magnetic permeability). The transfer of electrical currents in rocks occurs as conduction, electrolytic and surface conductivity. Ionic conduction occurs in rocks that contain free ion exchange; electrolytic conduction occurs in rocks filled with fluids in the pore spaces. Rocks behave as semi-conductors if they contain minerals, which are electrically semi-conducting.

Geothermal fields are usually associated with volcanic or intrusive sources. In a sedimentary basin, geothermal reservoirs may be due to sources located below the basin where the water taps heat from the source, and accumulates in the basin. The interaction of high temperature and rocks leads to mineral alteration. The assemblages of altered minerals equilibrate at a particular temperature. Therefore, the mineral assemblage caused by high-temperature fluids is located relatively close to the heat source (deep), and a low-temperature mineral assemblage occurs relatively far from the heat source (closer to the surface). The electrical conductivity is associated with electrolytic and surface electrical conduction of thermal water and the presence of clay minerals. Most clay minerals contain few ions such as Na^+, K^+, Ca^{2+}, Al^{3+}, Mg^{2+} Fe^{2+}, OH^- and H^+. Some clay minerals have a high coefficient of absorbing and retaining water. Other clay minerals do not have free ions and do not retain water for electrical current conductivity. Clay minerals formed at high temperatures are more resistive to electrical conduction (e.g. chlorite and epidote) than clay minerals formed as alteration of rocks at a lower temperature (e.g. smectite and zeolites). These properties are significant in the interpretation of electrical methods used for exploration of geothermal resources.

Wright et al. (2009) explain the dependency of porosity and electrical conductivity in volcanic rocks as conductivity increasing with increasing porosity. Permeability varies by several orders of magnitude in the volcanic crust and does not depend solely on porosity. Measurements of the electrical properties of saturated volcanic samples illustrate the influence of pathway tortuosity and pore shape on permeability. The differences are due to variations in the vesiculation and crystallization history. The vesicles in volcanic rocks reflect differences between explosive and effusive volcanic eruptions. Also, they reflect the relative ability of bubbles to form and maintain connected pathways during bubble expansion and collapse. Vesicular anisotropic rocks have high permeability and low electric tortuosity parallel to pore elongation, and low permeability and high electric tortuosity perpendicular to elongation.

If rocks contain significant amounts of highly conductive minerals such as leucite or magnetite, melting can lower the bulk conductivity as observed in the phonotephrite rocks, irrespective of the fact that conductivity is predominantly temperature dependent. Bulk chemical composition of a volcanic rock and its melt fraction play important roles; compositional parameters such as total alkali and total iron content greatly influence ionic and electronic conduction, respectively. An increasing melt fraction is more likely to increase bulk electrical conductivity (Poe et al., 2008).

2.3 Resistivity of rocks in high-temperature geothermal fields

Electrical resistivity or conductivity methods are more significant in the exploration of geothermal resources if the target is at considerable depth. The source of heat or a magmatic chamber may occur

at great depth depending on the crustal thickness and intrusions or volcanic eruptions in the area. The heat source can be located at depth, but the water convection cycle from the surface to the heat source and then back to the surface is the most important process, as it taps the heat from the heat source and brings it to the surface. The resistivity structure of the subsurface varies with depth depending on the geology (i.e. rock type, porosity, permeability and tectonics) of the area (Figure 2). One of the basic relationships is the occurrence of clay minerals in geothermal sources such as contact and low-grade metamorphism caused by hydrothermal water sources. Exploration and the interpretation of electrical geophysical methods have shown that the resistivity of rocks varies with temperature and pressure. Volcanic rocks, such as basalts, are composed of meso-stable minerals formed at a high temperature such as the Forsterite-Fayalite series, pyroxenes (ortho-pyroxene and para-pyroxene) and plagioclase rich in Ca^{2+} (anorthite). Hydrothermal alteration may add alkaline elements to form clay minerals. In volcanic rocks or basalts, the conductor is associated with altered clay minerals caused by hydrothermal water such as mixed clay layers (smectite-zeolites) or resistive layers caused by a chlorite-epidote clay layer. These kinds of geological environments lead to interpretations of a resistivity structure in relation to the geology, geothermal resources and the depth at which the geothermal sources are located.

Árnason et al. (1987a; 2000) discussed the resistivity structure of Icelandic high-temperature geothermal systems delineated by using electric and electromagnetic methods. Most high-temperature systems are within the basaltic crust and, therefore, have a similar resistivity structure. The resistivity structures are characterised by a low-resistivity cap at the outer margins of the reservoir, underlain by a resistive core. Resistivity is controlled by hydrothermally altered minerals, which are linked with the temperature distribution in the reservoir. At 100-220°C, low-temperature zones are dominated by smectite-zeolite minerals. At temperatures of 220-240°C, the zeolites disappear and smectite is replaced by chlorite. At temperatures exceeding 250°C, chlorite and epidote are the dominant alteration minerals. The electrical conductivity is explained by the presence of loose ions and a plate like crystal lattice structure of hydrated smectite, while in chlorite the cations are fixed. Because the mineral alteration is very dependent on temperature, the resistivity acts as a thermometer in high-temperature geothermal reservoirs, that is if the alteration is in equilibrium with temperature. Sometimes the area has cooled down and then the resistivity is a kind of maximum thermometer. The relationship between resistivity and hydrothermal alteration and temperature from the high-temperature geothermal field Nesjavellir is shown in Figure 2.

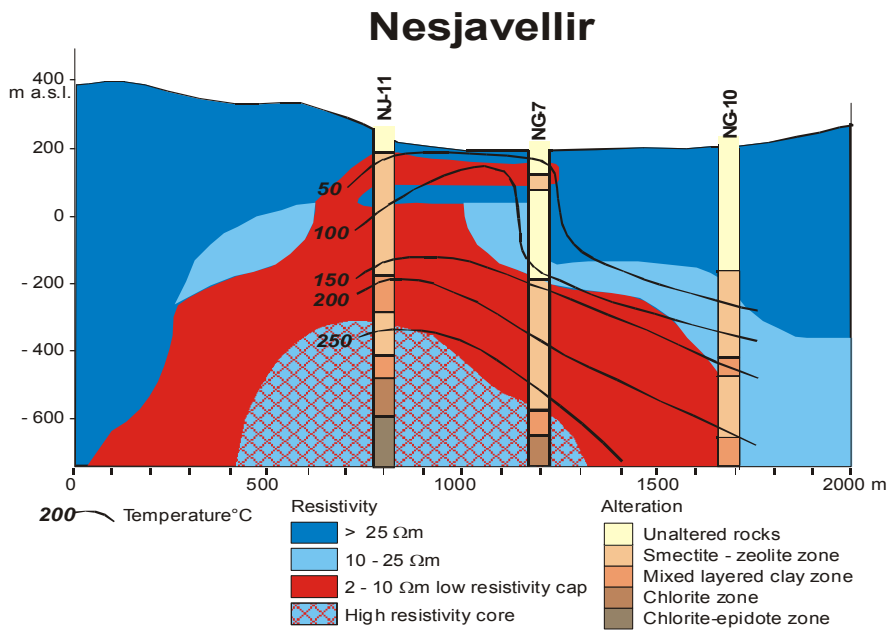

FIGURE 2: Resistivity cross-section from the Nesjavellir geothermal field, SW-Iceland, also showing alteration zoning in wells and temperature (Árnason et al., 1987b)

Spichak and Manzella (2009) explain that temperature is the major control of clay mineralogy. Chlorite, silicified zeolite and epidote clay minerals found in altered zones of volcanic rocks are related to low- and high-temperature geothermal activity. Below the cold, unaltered shallow part of the ground, the environment is characterised by low-temperature clay minerals such as smectite and

zeolites. Both are electrically conductive and formed at temperatures above 70°C. At higher temperatures, chlorite (more abundant in basaltic rocks) and/or illite (a less conductive clay mineral in acidic rocks) may appear, inter-layered with low-temperature alteration minerals. The amount of chlorite or illite increases with temperature, especially at temperatures above 180°C. Zeolite and smectite disappear at 220-240°C and pure chlorite and/or illite usually appear at temperatures higher than 240°C, along with other high-temperature alteration minerals such as epidote in propylitic alteration assemblages (Henn et al., 2007). The general chlorite formula is given by $[(R^{2+}, R^{3+})_6, (Si, Al)8O_{20}, (OH)_4][(R^{2+}, R^{3+})_6(OH)_{12}]$; the first is talc-like, the second member brucite-like sheets, R^{2+} is the sum of the divalent cat ions (Mg, Fe), and R^{3+} is the sum of the trivalent cat ions (Al, Fe). When Al replaces Si in a tetrahedral sheet, an excess of negative charge occurs. These negative apparent charges can be balanced by the positive apparent charges, which are created by the replacement of R^{2+} by R^{3+} in octahedral sheets (either in the brucitic or in the talc-like sheet). The resulting charges can be low or null, and this explains the low amount of compensating charge, and thus the low cation exchange capacity value for chlorites. In addition to this low but intrinsic charge present in the bulk of the crystallographic structure, a variable charge is common to all mineral surfaces. The dependency of resistivity of water on depth (pressure) and temperature is summarised in Figure 3. The resistivity of water decreases with increasing temperature as the mobility of ions increases due to a decrease in viscosity. At temperatures up to 150-200°C, the resistivity can be described by the relationship expressed in Equation 16 (Dakhnov, 1962; Hersir and Björnsson, 1991):

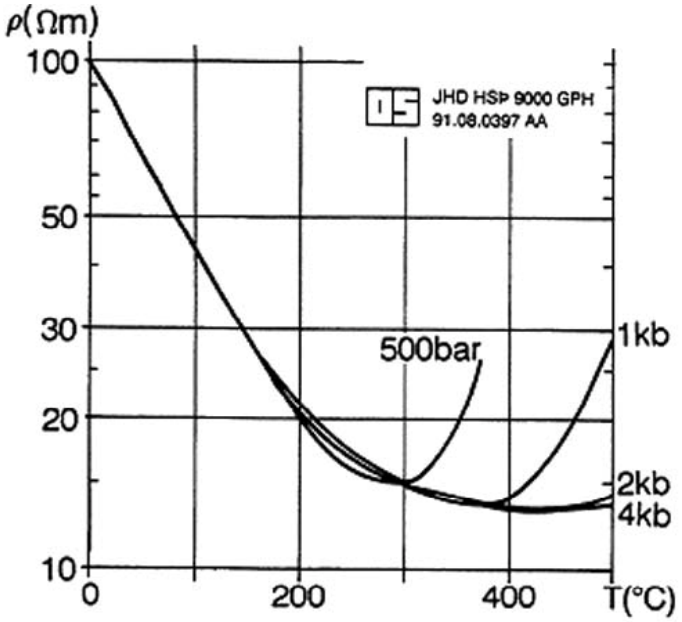

FIGURE 3: Electrical resistivity as a function of temperature at different pressures (Hersir and Björnsson, 1991; Zhdanov and Keller, 1994)

$$\rho_w = \rho_{w0} / (1 + \alpha(T - T_0)) \quad (16)$$

where ρ_{w0} = Resistivity of the fluid at the reference temperature (Ωm);
T_0 = Reference temperature (°C);
α = Temperature coefficient of resistivity, around 0.023 $°C^{-1}$ for $T_0 = 23°C$.

At higher temperatures, a decrease in the dielectric permittivity of water results in a decrease of disassociated ions and an increase in fluid resistivity.

3. MAGNETOTELLURIC AND TRANSIENT ELECTROMAGNETIC METHODS

This part describes the magnetotelluric (MT) method, which uses natural (passive) electromagnetic sources and the transient electromagnetic (TEM) method, which uses a small loop controlled source. Although the MT and TEM methods are in many ways different, they have the common property of measuring the electrical conductivity distribution with depth. Both methods use secondary electromagnetic signals. The TEM does not experience static shift while the MT does. Both methods are cost effective in exploring geothermal resources.

3.1 The transient electromagnetic (TEM) method

The transient electromagnetic method uses a controlled source transmitter and a receiver. TEM can use a central loop (inloop) layout, a coincident loop or a displaced loop to probe the conductivity structure of the Earth (Figure 4). The TEM method uses induced currents in the ground caused by primary electromagnetic waves from a transmitter loop. The central loop layout is effective in measuring the vertical component of the induced electromagnetic signatures. Therefore, the central loop configuration is best for vertical resistivity measurements.

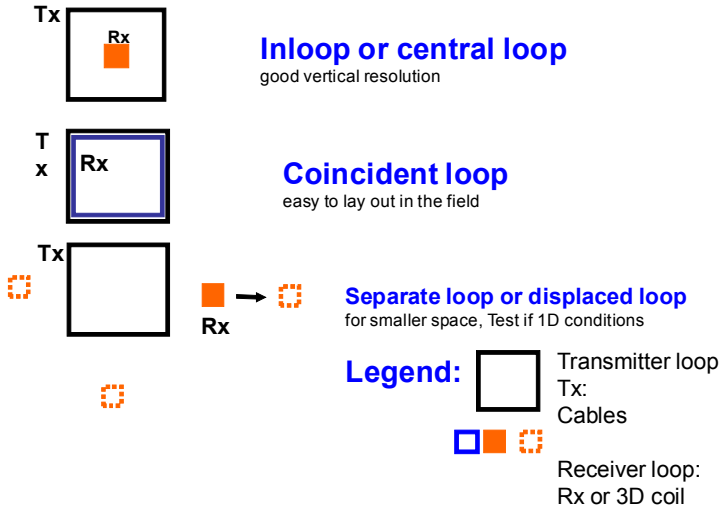

FIGURE 4: Different configuration layout for the TEM method

The TEM method is less expensive, requires a smaller work force, and interpretations of data is less time consuming than that of Schlumberger soundings. Also, TEM responses focus more downwards. The TEM method does not require a current being injected into the Earth; therefore, the method can be used in all accessible environments such as on snow, rugged mountains and dry sand surface without affecting the electromagnetic signatures. The interpretation of TEM is mainly 1-D, as a vertical sounding. The combination of several soundings along a profile may give 2-D variations of the subsurface.

Árnason (1989) and Spichak and Manzella (2009) show how to conduct TEM measurements using the central loop (inloop) layout. The decaying magnetic field is measured as a function of time in a spool or a receiver coil and the transmitted current is measured as well. The loop may be a square, a circle or a rectangle in shape but the square loop configuration is most convenient for fieldwork. The transmitter is switched on as the electromagnetic signal is transmitted and then abruptly switched off and the receiver detects the signals from the ground (Figure 5). Measurements are taken after the current has been turned off in the transmitter. The sampling time, signal amplifications, repetition rates (frequency) and turn off time are synchronised between the transmitter and receiver. First, a constant current is transmitted into the loop to generate a constant magnetic field of known strength around the loop, induced into the ground. Once the current is switched off, the decaying magnetic field induces electrical currents into the ground to compensate for the effects. The induced electrical field, on the other hand, produces a secondary magnetic field decaying with time. The production of the secondary electromagnetic fields in the absence of primary sources is called a transient electromagnetic wave (TEM). The decay rate of the secondary magnetic field is monitored by measuring the voltage induced in the receiver coil. For repeated measurements of the subsurface response, the transmitter has to be switched off and on at a set interval.

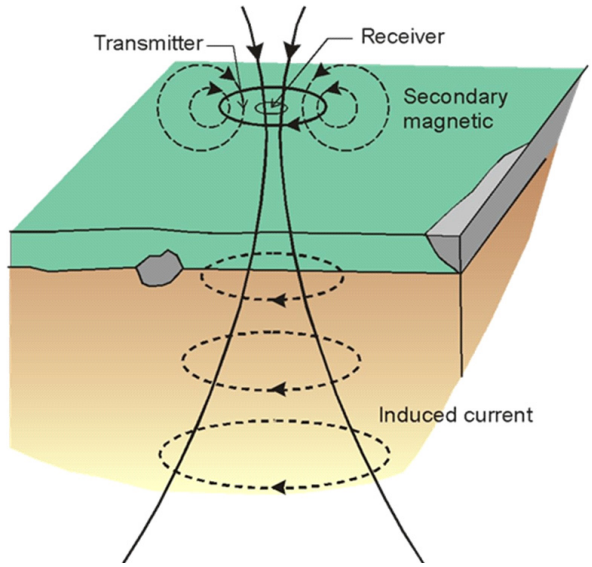

FIGURE 5: The central loop TEM sounding configuration

After switching off the current source, the ground/subsurface, which has been experiencing a primary magnetic field, generates a secondary current to compensate for the primary current. At an early time, the secondary electrical properties will behave almost like the current in the loop but later, the secondary current reflects the subsurface physical properties. The induced magnetic field and the induced eddy currents in the formation counteract and propagate downwards with time (Figures 5 and 6). In these processes, the primary magnetic field decays logarithmically with time and the subsurface layers generate secondary electrical and magnetic fields.

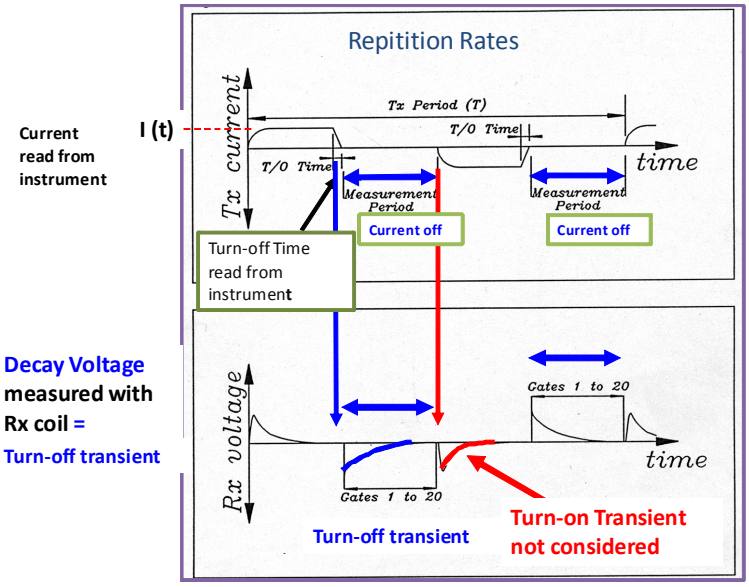

FIGURE 6: Transmission and decaying of signals

The transmission of TEM signals can be envisioned as spikes that occur repeatedly with time. The response of the magnetic moment depends on the distance from the spike point of pulses to the ground. The response of the ground is detected at a distance between the signal transmission and the receiver. The strength of the magnetic dipole moment depends on the current, the loop type, the cable cross-sectional area, the size of the loop and the number of windings.

The following are a few steps developed by Árnason (1989) in estimating the resistivity of the subsurface by considering the magnetic dipole moment, expressed in Equation 17.

$$\boldsymbol{M} = \boldsymbol{M}_0 e^{i\omega t}\boldsymbol{z}\delta(x - x_0) \tag{17}$$

$\boldsymbol{M}$ is the magnetic moment at point x, the source dipole is located at x_o at a given time, $\boldsymbol{M}_o$ is the initial magnetic dipole moment, **z** is a unit vector and δ is the Dirac's delta function.

The product of the generated electric field, the radius of the loop and the number of turns in the loop using a central loop configuration, give the voltage response in the receiver coil as:

$$V_c = 2\pi n_r r_c E(r_c) = A_r n_r \frac{2E(r_c)}{r_c} \tag{18}$$

The mutual coupling of the measured voltage in the receiver coil and the transmitted current in the source loop defines the mutual impedance of the subsurface as expressed in Equation 18:

$$Z_c(r,\omega) = \frac{V_c}{I_0 e^{i\omega t}} = A_r n_r A_s n_s \frac{-i\omega\mu_0}{\pi r}\int_0^\infty \frac{\lambda^2}{m_0}\frac{S_0}{S_0 - T_0}J_1(\lambda r)d\lambda \tag{19}$$

The Fourier expansion of the transmitted current function *I(t)* gives:

$$I(t) = \frac{1}{(2\pi)^{1/2}}\int_{-\infty}^{\infty}\tilde{I}(\omega)e^{i\omega t}d\omega \tag{20}$$

where $$\tilde{I}(\omega) = \frac{1}{(2\pi)^{1/2}} \int_{-\infty}^{\infty} I(t) e^{-i\omega t} dt$$

The response of the measured voltage in terms of the mutual impedance as a function of time is:

$$V_c(t,r) = \frac{1}{(2\pi)^{1/2}} \int_{-\infty}^{\infty} Z_c(\omega,r)\tilde{I}(w) e^{i\omega t} d\omega \quad (21)$$

As mentioned before, the induced voltage or currents at an early time, just after the current is switched off, behaves similarly to the current in the loop. The ground surface near the loop experiences this phenomenon.

At later time, the electrical field penetrates deeper into the subsurface; the induced voltage decreases linearly as its slope is equivalent to $t^{-5/2}$. The following equation defines the so-called late time apparent resistivity of the TEM.

$$\rho_a = \frac{\mu_0}{4\pi}\left[\frac{2\mu_0 A_r n_r A_s n_s}{5t^{5/2} V_c(rt)}\right]^{2/3} \quad (22)$$

3.2 The magnetotelluric (MT) method

The magnetotelluric (MT) method uses time variations of the Earth's natural electromagnetic fields to determine the electrical conductivity of the Earth. The solar system ejects charged particles called solar winds. These particles are mainly protons and electrons interacting with the Earth's magnetosphere and produce electromagnetic fields. The charges in the ionosphere cause displacement currents and conduction currents. Lightning and thunderstorms are produced by conduction currents. The flow of charged particles in ionospheric zones or magnetospheric layers as hydromagnetic waves or plasma, generates electrical and magnetic fields that propagate towards the Earth (Vozoff, 1991). The strength of the electromagnetic fields depends on time and position (in latitude) due to the solar-Earth rotation relationship and the ejection of the Earth's magnetic field. The magnetic field of the Earth varies from the equator to the poles. The interactions of solar particles and the Earth's magnetic fields result in electromagnetic waves of various frequencies. When reaching the ground, the electromagnetic waves penetrate to great depths and interact with subsurface layers that produce secondary electromagnetic fields that are measured by the MT instruments.

The MT method is capable of investigating the electrical conductivity of the subsurface from a few metres below the surface to a depth of hundreds of kilometres, or to the upper mantle. The skin depth (depth of penetration or depth of investigation) is the depth at which the electromagnetic wave is reduced to e^{-1} of its original value. The depth of penetration or the skin depth depends not only on the frequency of the electromagnetic field but also on the conductivity (resistivity) of the medium in which the wave propagates. For a fixed period, the skin depth increases with increasing resistivity of the subsurface.

All MT methods use passive electromagnetic fields except the Radiomagnetotelluric (RMT) and Controlled Source Audiomagnetotelluric (CSAMT) methods, which use controlled sources (Zonge and Hughes, 1991). The RMT method uses EM fields transmitted from remote radio stations at the frequency range of 20 to 200 kHz. It has a depth of investigation that ranges from 1 to 100 m. The AMT method uses electromagnetic sources ranging from 0.1 to 10 kHz. The source of the electromagnetic fields is associated with thunderstorms and lightning mainly found in tropical or equatorial regions. On the other hand, the AMT method has a shallow to medium depth of investigation even though it may penetrate to depths ranging from a few metres to a few kilometres.

The MT and Long period magnetotelluric method (MT-LMT) uses periods in the range of 1-100,000 s (Smirnov et al., 2008). Therefore, prior to MT surveys, one must first select the MT instruments according to the characteristics and the objectives of the survey.

In the MT method, electric and magnetic sensors measure the time variations of the magnetic and electrical fields. The sensors are buried at shallow depths in the ground. Electrical fields are measured by using two perpendicular electrical dipoles in N-S and E-W directions. The electrical component in N-S is denoted as E_x and the E-W component as E_y. The magnetic components are oriented in the N-S direction, denoted as H_x and in the E-W direction, denoted as H_y. H_z is the vertical component. The data are recorded in a digital format (Figure 7). The only filter that is used prior to recording is an anti-aliasing filter. By using two MT instruments separated by a short distance (less than 1 km) it is, in most cases, sufficient to measure only the two electrical components at one of the stations. The two component instruments use the magnetic components from the nearby station for computing the subsurface impedances.

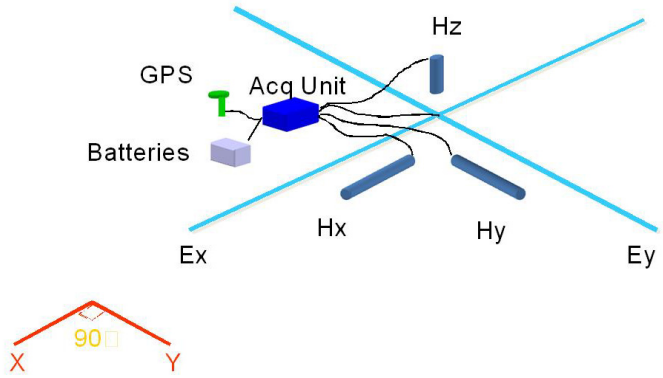

FIGURE 7: Setup of MT instruments

In the MT method, electromagnetic signals are recorded as a time series, and are then transformed to the frequency domain by using the Fourier transformation technique. Real Time Analysis takes place at the site during data acquisition and involves the selection of several parameters such as the orientation of the coils, the electrical dipole separation and orientation, the filters selection (e.g. anti-aliasing), the sampling period/frequency, the initial and final sampling time, calibrations, and synchronization of the remote reference station. The Fast Fourier Transform (FFT) transforms the Time Series data to the frequency domain. The anti-aliasing filters are used prior to digital recording in order to prevent aliasing. The curves of the impedances, apparent resistivities and phases, etc. are plotted to infer the electrical resistivity distribution with depth (see examples in the Appendices). The technique of maximising the signal to noise ratio and the computation of the impedance components the MT data are both discussed in Section 3.3.

The main objective of using the MT method is to estimate conductivity variations with depth. Zonge and Hughes (1991), Zhdanov and Keller (1994) and Simpson and Bahr (2005) have shown the depth estimation of the MT method. The depth of penetration can be estimated by calculating the values of the wave propagation constant, k (from Equations 11 and 12) using the following equation:

$$k^2 = \mu\varepsilon\omega^2 - i\mu\sigma\omega \tag{23}$$

The conductivity of the subsurface is in the range $1\text{-}10^{-4}$ S/m and the frequencies used are less than 10^3 Hz. Using the values of the magnetic permeability and dielectric permittivity, it is easily seen that Equation 23 can be simplified into the quasi-stationary approximation:

$$k^2 = -i\mu\sigma\omega \tag{24}$$

Zonge and Hughes (1991) have shown that the propagation constant *k* is a complex number that can be written as:

$$k = (\alpha - i\beta) = [-i\mu\omega(\sigma + i\omega\varepsilon)]^{\frac{1}{2}} \tag{25}$$

The phase constant α is given by:

$$\alpha = \omega \left[\frac{\mu\varepsilon}{2} \left(\sqrt{1 + \left(\frac{\sigma}{\varepsilon\omega} \right)^2} + 1 \right) \right]^{\frac{1}{2}} \tag{26}$$

The attenuation constant β is given by the equation:

$$\beta = \omega \left[\frac{\mu\varepsilon}{2} \left(\sqrt{1 + \left(\frac{\sigma}{\varepsilon\omega} \right)^2} - 1 \right) \right]^{\frac{1}{2}} \tag{27}$$

The skin depth δ is defined as:

$$\delta = {}^{1}/_{\beta} \tag{28}$$

The relationship of wavelength λ, propagation velocity v_p, and frequency f of the signal is given in Equations 29-31:

$$\lambda = 2\pi\delta \tag{29}$$

$$v_p = f\lambda \tag{30}$$

$$\omega = 2\pi f \tag{31}$$

The velocity of electromagnetic waves is a constant, 3×10^8 m/s. Therefore, the skin depth depends only on the frequency or the wavelength and the resistivity structure of the subsurface. The quasi-stationary approximation of Equation 25 simplifies to Equation 32, assuming that the subsurface conductivity is much higher than the product of the angular frequency and the dielectric permittivity, $\sigma >> \varepsilon\omega$:

$$k = (1 - i)\sqrt{\frac{\mu\sigma\omega}{2}} \tag{32}$$

$$\beta = \frac{1}{\delta} = \sqrt{\omega\mu\sigma/2} \tag{33}$$

$$\delta = \sqrt{\frac{2}{\mu\sigma\omega}} = 503\sqrt{\frac{\rho}{f}}\ \ metres \tag{34}$$

Equation 34c, still gives two unknown parameters, conductivity σ, and skin depth δ. Of the two parameters, only the conductivity can be calculated from the impedances. The impedances can be calculated from the electrical and magnetic fields measured in the uppermost layer.

Stoldt (1981) has shown the relationship between the impedance and the admittance using the electrical and magnetic fields. Equation 35 defines the impedance of the subsurface as the ratio between the horizontal and perpendicular electrical and magnetic fields.

$$Z_{xy} = \frac{E_x}{H_y} \tag{35}$$

The relative frequency impedance is a complex number and its magnitude is:

$$|\boldsymbol{Z}| = \sqrt{|Z_{Re}^2| + |Z_{Im}^2|} \tag{36}$$

The direction of the complex vector, the phase, is

$$\theta = tan^{-1}\left|\frac{Z_{Im}}{Z_{Re}}\right| \tag{37}$$

In anisotropic conditions, the conductivity distribution in a given layer is the ratio between the electric current density and the electric field denoted in a matrix form as anisotropic distributions of electric conductivity

$$\begin{bmatrix} j_x \\ j_y \\ j_z \end{bmatrix} = \begin{bmatrix} \sigma_{xx} & \sigma_{xy} & \sigma_{xz} \\ \sigma_{yx} & \sigma_{yy} & \sigma_{yz} \\ \sigma_{zx} & \sigma_{zy} & \sigma_{zz} \end{bmatrix} \begin{bmatrix} E_x \\ E_y \\ E_z \end{bmatrix} \tag{38}$$

The impedance tensor (***Z***) is

$$\begin{bmatrix} E_x \\ E_y \end{bmatrix} = \begin{bmatrix} Z_{xx} & Z_{xy} \\ Z_{yx} & Z_{yy} \end{bmatrix} \begin{bmatrix} H_x \\ H_y \end{bmatrix} \tag{39}$$

The admittance tensor (***Y***) is

$$\begin{bmatrix} H_x \\ H_y \end{bmatrix} = \begin{bmatrix} Y_{xx} & Y_{xy} \\ Y_{yx} & Y_{yy} \end{bmatrix} \begin{bmatrix} E_x \\ E_y \end{bmatrix} \tag{40}$$

The impedance is the reciprocal of the admittance.

$$\boldsymbol{Z}=\boldsymbol{Y}^{-1} \tag{41}$$

Vozoff (1991) has shown the relationship between resistivity ρ or conductivity σ and impedance as given in Equations 23 and 35. Since the measured parameters are the electrical and magnetic fields, resistivity of the subsurface based on the impedance can be computed using Equation 35:

$$\boldsymbol{H} = \frac{k}{\omega\mu}\hat{\boldsymbol{n}}x\boldsymbol{E} \tag{41}$$

where $\hat{\boldsymbol{n}}$ is the unit vector pointing vertically downwards, and k is the wave propagation constant.

$$Z_{xy} = \frac{\mu\omega}{k} = (1+i)\sqrt{\frac{\rho\omega\mu}{2}} \tag{42}$$

$$\rho_{xy} = \frac{Z_{xy}Z_{xy}^*}{\mu\omega} = \frac{1}{\omega\mu}\left|\frac{E_x}{H_y}\right|^2 = \frac{1}{5f}\left|\frac{E_x}{H_y}\right|^2 \tag{43}$$

Equation 43 gives us freedom to calculate the resistivity from three recorded parameters (f, H_i and E_j). Since the Earth is not homogeneous, conductivity is not a constant. The conductivity may vary horizontally and vertically and produce 1-D, 2-D and 3-D structures. Conductive structures such as faults and fissures often produce a two-dimensional resistivity model (2-D). In 2-D models, the conductivity of the subsurface varies in one horizontal direction plus the vertical direction (e.g. the x-direction and the z-direction). 3-D models assume that the electrical resistivity structure differs in all directions. The variations of the conductivity structure can be analysed based on the skew, rotation

angle, and the impedance tensor elements Z_{xx} Z_{yy} Z_{xy} and Z_{yx}. Zhang et al. (1987) summarize the characteristics of 1-D and 2-D models based on the impedance ratio. In 1-D models, the values Z_{xx} and Z_{yy} are equal to zero and the intermediate impedances Z_{yx} and Z_{xy} are equal but have opposite signs, or:

$$\begin{bmatrix} Z_{xx} = Z_{yy} = 0 \\ Z_{xy} = -Z_{yx} \neq 0 \end{bmatrix} \tag{44}$$

The vertical magnetic field component is linearly related to the horizontal magnetic fields. Zhdanov and Keller (1994) have shown the Weiss-Parkinson relationship:

$$H_z = T_x H_x + T_y H_y \tag{45}$$

The element T_i is known as the tipper; it is complex since it may include phase shifts. The tipper can be used in the interpretation of 2-D structures. If the strike is in the x-direction, the relationship simplifies to Equation 46:

$$H_z = T_y' H_y' \tag{46}$$

3.3 Reduction of MT data

MT data are recorded as a time series. They are sampled as a time series and then transformed to the frequency domain through a Fourier transformation (Hermance, 1973). Anti-aliasing filters are used to prevent aliasing. A proper setup of the instrument in the field reduces or minimises noise in magnetotellurics. A field MT setup tends to avoid possible sources that could cause vibrations in the electrical dipole cables, magnetic coils cables or any possible influence from an external electromagnetic field to the system (cultural noise). The use of a remote reference station during data acquisition is another way of reducing uncorrelated noise (Figure 8). All kinds of noise such as wind or any source of vibrations may also affect the telluric signal and introduce a noise level in the measurements.

3.3.1 Spectral power density analyses

Spectral power density analyses are used to maximise the signal to noise ratio. Spectral power density analyses in the magnetotelluric method make use of either a synchronized remote reference or data from a single site. The remote reference station is located several tens of kilometres away from the measuring site. The technique reduces uncorrelated noise. Noise not correlated in both stations becomes zero when making an auto power density analysis of the fields. Impedances calculated by auto or cross power density spectral analysis suggest that magnetic fields are more stable; thus, it is preferable to use them with electrical or magnetic fields in a spectral density analysis. To avoid correlating errors, the cross power density analysis uses a remote reference, more suitable than an auto power density analysis from a single site. Simpson and Bahr (2005) explained the spectral density analyses using both a single station and a remote reference as shown in Equations 48-50. Equation 24 contains some errors due to noise; it can be written as follows:

$$E_x = Z_{xx} H_x + Z_{xy} H_y \tag{47a}$$

$$E_y = Z_{yx} H_x + Z_{yy} H_y \tag{47b}$$

The spectral density analyses multiply the tensors by the electric or magnetic conjugate fields. The combinations of the magnetic fields, electrical fields and impedance tensors give eight equations (e.g. Wight et al., 1977 and Zhang et al., 1987); two equations are shown here as examples:

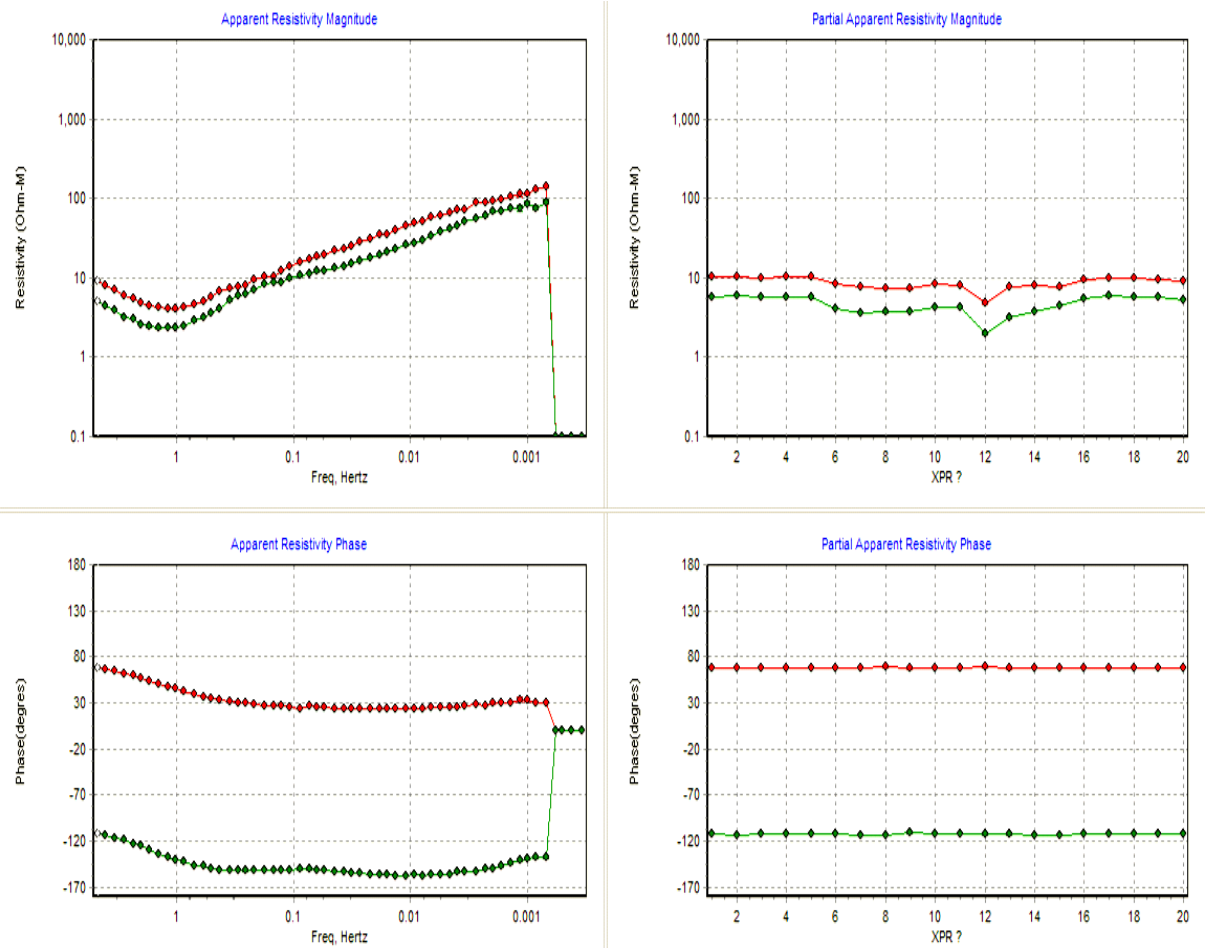

FIGURE 8: Apparent resistivity and phase curves for both directions as a function of frequency after noise reduction (left part) and the partial resistivity and phase for a certain frequency (right part)

$$E_x E_x^* = Z_{xx}\langle H_x E_x^*\rangle + Z_{xy}\langle H_y E_x^*\rangle \tag{48a}$$

$$E_x E_y^* = Z_{xx}\langle H_x E_y^*\rangle + Z_{xy}\langle H_y E_y^*\rangle \tag{48b}$$

The products of the magnetic and electrical field spectra using the tensor elements give eight equations. To remove the bias, a remote reference is used to eliminate uncorrelated noise. The impedances Z_{ij} are computed using the following equations:

$$Z_{xx} = \frac{\langle \bar{N}\bar{X}_r^*\rangle\langle \bar{Y}\bar{Y}_r^*\rangle - \langle \bar{N}Y_r^*\rangle\langle \bar{Y}\bar{X}_r^*\rangle}{DET} \tag{49a}$$

$$Z_{xy} = \frac{\langle \bar{N}\bar{Y}_r^*\rangle\langle \bar{X}\bar{Y}_r^*\rangle - \langle \bar{N}\bar{X}_r^*\rangle\langle \bar{X}\bar{Y}_r^*\rangle}{DET} \tag{49b}$$

$$Z_{yx} = \frac{\langle \bar{E}\bar{X}_r^*\rangle\langle \bar{Y}\bar{Y}_r^*\rangle - \langle \bar{E}Y_r^*\rangle\langle \bar{Y}\bar{X}_r^*\rangle}{DET} \tag{49c}$$

$$Z_{yy} = \frac{\langle \bar{E}\bar{Y}_r^* \rangle \langle \bar{X}\bar{Y}_r^* \rangle - \langle \bar{E}\bar{X}_r^* \rangle \langle \bar{X}\bar{Y}_r^* \rangle}{DET} \tag{49d}$$

where

$$DET = \langle \bar{X}X_r^* \rangle \langle \bar{Y}\bar{Y}_r^* \rangle - \langle \bar{X}\bar{Y}_r^* \rangle \langle \bar{Y}\bar{X}_r^* \rangle \tag{50}$$

3.3.2 Static shift in the magnetotelluric method

MT signatures can experience pronounced static shift. The static shift is due to patterns and inhomogeneity in the near-surface geological structure of the area. Electric fields shift towards high conductive bodies/structures while the magnetic field tends to be stable. The static shift multiplier from one site to another is generally unknown but assumed to be random, which is not always the case. For this reason, the multiplier factors differ from site to site. The increase or decrease in electrical components tends to increase or lower the impedance tensors. Generally, magnetotelluric fields tend to shift vertically. Static shift causes changes in the apparent resistivity structure by a scale factor that leads to erroneous results.

Berdichevsky (1999) outlines two kinds of magnetotelluric dispersions: the magnetotelluric dispersion which occurs between the real and imaginary parts of the impedance, and the dispersion between apparent resistivity ρ and impedance phase φ. The dispersion relationships of the first kind take the form:

$$R(\omega_0) = \frac{2}{\pi} pv \int_0^\infty \frac{X(\omega)}{\omega^2 - \omega_0^2} \omega d\omega \tag{51}$$

The dispersion relationships of the second kind are in the form of:

$$\varphi(\omega_0) = -\frac{\pi}{4} - \frac{\omega_0}{\pi} pv \int_0^\infty ln\, \rho_A(\omega) \frac{d\omega}{\omega^2 - \omega_0^2} \tag{52}$$

Sternberg et al. (1988) described a method for correcting static shift in the magnetotelluric method by incorporating the electromagnetic sounding from the same vicinity. The TEM sounding should be very close to or at least less than 100 m from the MT site. TEM has no static shift effects due to near-surface inhomogeneities because it does not monitor the electrical field. Here, the static shift is corrected through a joint inversion of TEM and MT soundings, using the inversion program TEMTD developed by Árnason (2006).

4. QUANTITATIVE INTERPRETATION OF TEM AND MT

Quantitative interpretation of geophysical data tries to estimate the vertical and horizontal extension of the geological bodies that cause a certain anomaly. Characterisation of geological features requires known petrophysical parameters related to the method applied. The main physical parameters that link the geological features and electrical signatures are rock conductivities, permeability and dielectric permittivity. The electrical properties or parameters may vary due to mineral content, porosity and permeability and tectonic shearing. Shearing, alteration and secondary mineralization may increase or reduce physical properties of rocks such as the permeability (Chiragwile, 2007). Inhomogeneities of physical parameters provide information on rock properties, thermodynamics and the phase composition of rocks at great depth. The information is useful in regional prediction of prospective minerals and energy resources (Zhdanov and Keller, 1994).

Interpretations of TEM and MT electromagnetic data aims at the delineation of electrical resistivity structures. The inversion of MT and TEM data is accomplished by using developed computational algorithms, for 1-D to estimate depth, thickness and the corresponding physical characteristics. The useful physical parameters in TEM and MT are the conductivity or resistivity of the body, magnetic permittivity and dielectric constants. However, among the aforementioned parameters, permeability and dielectric permittivity contribute less than conductivity to the electromagnetic fields' diffusion; therefore, they are not used.

There are two known approaches to interpreting TEM and MT data: forward (numerical) modelling and inversion modelling (misfit of calculated and observed signals). The inversion modelling approach uses the misfit technique of the two curves of calculated and measured data. The inverse modelling is easier and faster compared to forward modelling. The best estimate is found once the calculated (assumed) and measured (observed) curves fit reasonably well. For 1-D interpretation, the curves are aligned by changing the parameters such as the number of layers, the thickness of layers, and the conductivity properties. For geoelectrical methods, the most widely used inversion method is the non-linear least square method (Árnason, 1989). It estimates that the residue of the best fit relates to the sum of the residue square and the probability of the normal distribution curve.

Another approach in interpreting MT data defines the strike direction of the electrical conducting structure. TEM is limited to 1-D because of the downward focusing behaviour while MT focuses on one, two or even three dimensions. In order to view a 2-D structure in TEM, the survey programme needs several measurements taken on a profile from which the inverted 1-D interpreted data appears as a resistivity pseudo-section (2-D). Since MT data depend on the resistivity structure, it is possible to view the variations in impedance tensors (Z_{xx}, Z_{yy}, Z_{xy} and Z_{yx}) that define the dimensional property of the resistivity structure from the site. For MT measurements from a homogeneous 1-D structure, the plots of the impedances Z_{xy} and Z_{yx} against periods tend to correlate simultaneously. For the inhomogeneous structure and non 1-D model structures, the plots of the impedances Z_{xy} and Z_{yx} against periods tend to deviate at discontinuities. The strike trends of the conductive structure orient at an angle at which the absolute values Z_{xy} and Z_{yx} are maximal and the absolute values of Z_{xx} and Z_{yy} are minimal or zero (refer to Equation 44). Vozoff (1991) and Simpson and Bahr (2005) showed that the estimation of the rotation angle estimates the strike direction of a 2-D resistivity structure. The angle of rotation used to estimate the strike assumes that the instruments are oriented in a NS and EW direction making an angle θ with the conductor structure as shown in the following relationships.

$$\boldsymbol{E'} = \boldsymbol{M_\theta E} \tag{53}$$

$$\boldsymbol{B'} = \boldsymbol{M_\theta E} \tag{54}$$

$$\boldsymbol{Z'} = \boldsymbol{M_\theta Z M^T} \tag{55}$$

$\boldsymbol{M_\theta}$ is the rotation matrix, $\boldsymbol{E'}$, $\boldsymbol{B'}$ and $\boldsymbol{Z'}$ are the electrical and magnetic fields and the impedance, respectively, after rotation, $\boldsymbol{M^T}$ is the transpose matrix of $\boldsymbol{M}$.

Inversion modelling, used in this study, is based on the non-linear least square method. The best fit between the calculated and observed measurements is obtained when x^2 is minimal or zero (Árnason, 1989; Simpson and Bahr, 2005):

$$x^2(b) = \sum\left(y_{0i} - f(x_i, b)\right)^2 / \sigma_i^2 \tag{56}$$

The first and second derivatives give the minimum points at which x^2 is zero (turning points). To fit the curves an inversion algorithm is used. The potential function is minimised by:

$$Pot = x^2 + \alpha^* DS_1 + \beta^* DS_2 + y^* DD_1 + \delta^* DD_2 \tag{57}$$

where DS_1 and DS_2 are the first and second order derivatives of log-conductivities in the layered model and DD_1 and DD_2 are the first and second order derivatives of logarithms of the ratios of layer depths. The coefficients α, β and γ are the relative contributions of the different damping terms. Figures 9 and 10 show an example of the iterative inversion of a TEM sounding and a joint inversion of the MT and TEM sounding, respectively.

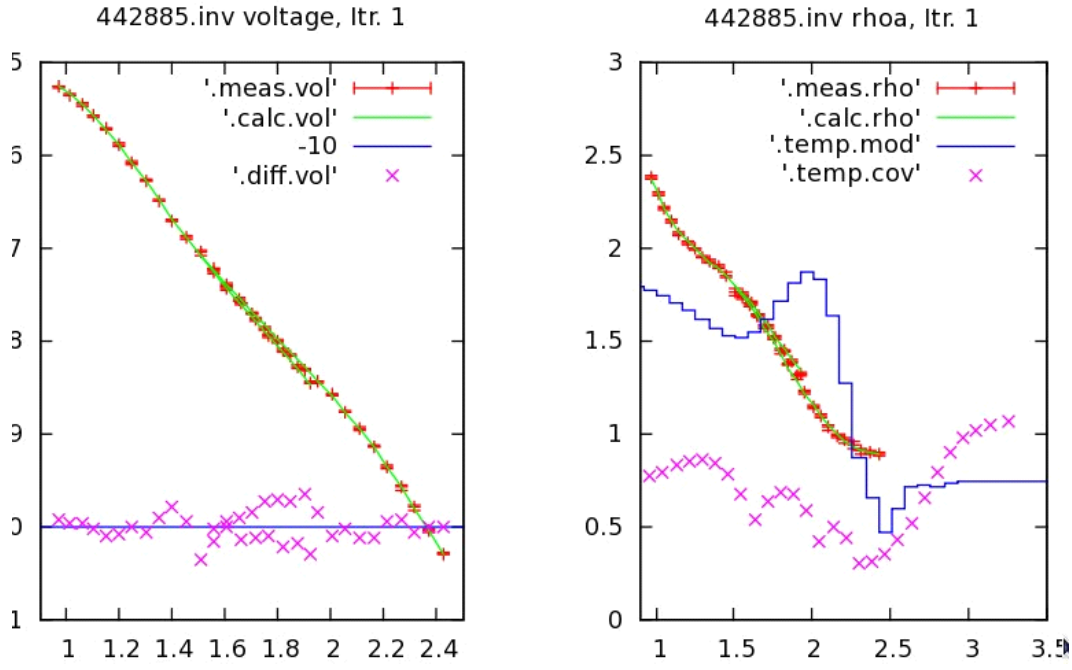

FIGURE 9: Inversion of TEM data

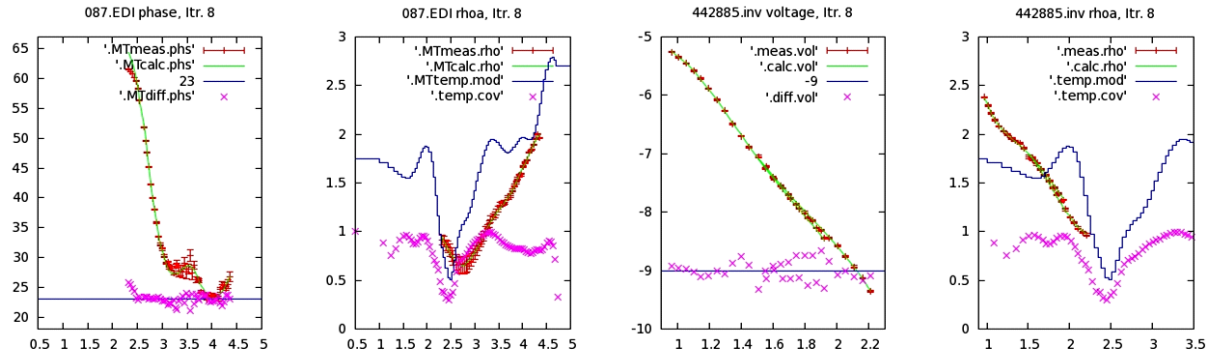

FIGURE 10: Inversion of MT and TEM data (TEMTD)

In addition to the geophysical approach, the integration of geological, geochemical and physical parameters, geological maps, fluid chemistry, lithological stratigraphy, and temperature logs with depth from drill holes are important in the interpretation of geothermal energy resources.

5. RESISTIVITY STRUCTURE OF THE KRÝSUVÍK GEOTHERMAL FIELD

A joint inversion was done on TEM and MT data on a profile that crosses some of the main geological structures of the Krýsuvík geothermal system. The results were compared with geological data from boreholes. The TEM and MT data used in this report were part of an extensive survey conducted during the last decade (Hersir et al., 2009). HS Orka permitted the use of the data.

5.1 Geology of Iceland and the Krýsuvík high-temperature geothermal field

Iceland is located on the Mid-Atlantic Ridge inferring that the composition of the rocks is mainly basaltic. The four main rock formations are classified as the Upper Tertiary-Plateau basalt formation, the Upper Pliocene and Lower Pleistocene grey basalt formation, the Upper Pleistocene palagonite (hyaloclastite) móberg formation and the Postglacial formation. The Postglacial formation consists of basaltic lavas and sediments, such as till and glacial sediments from the retreat of the last ice cover, and marine, fluvial and lacustrine sediments and soils of Late Glacial and Holocene age. Tillite strata separate the Postglacial hyaloclastite and interglacial lava deposits. The Mid-Atlantic Ridge crosses the country from the southwest through the middle of the country and up through the north, and, expressed on land, through the active volcanic rift zone. Associated with the active volcanic systems are high-temperature geothermal areas (Figure 11), one being the Krýsuvík high-temperature geothermal field located in SW-Iceland on the Reykjanes Peninsula.

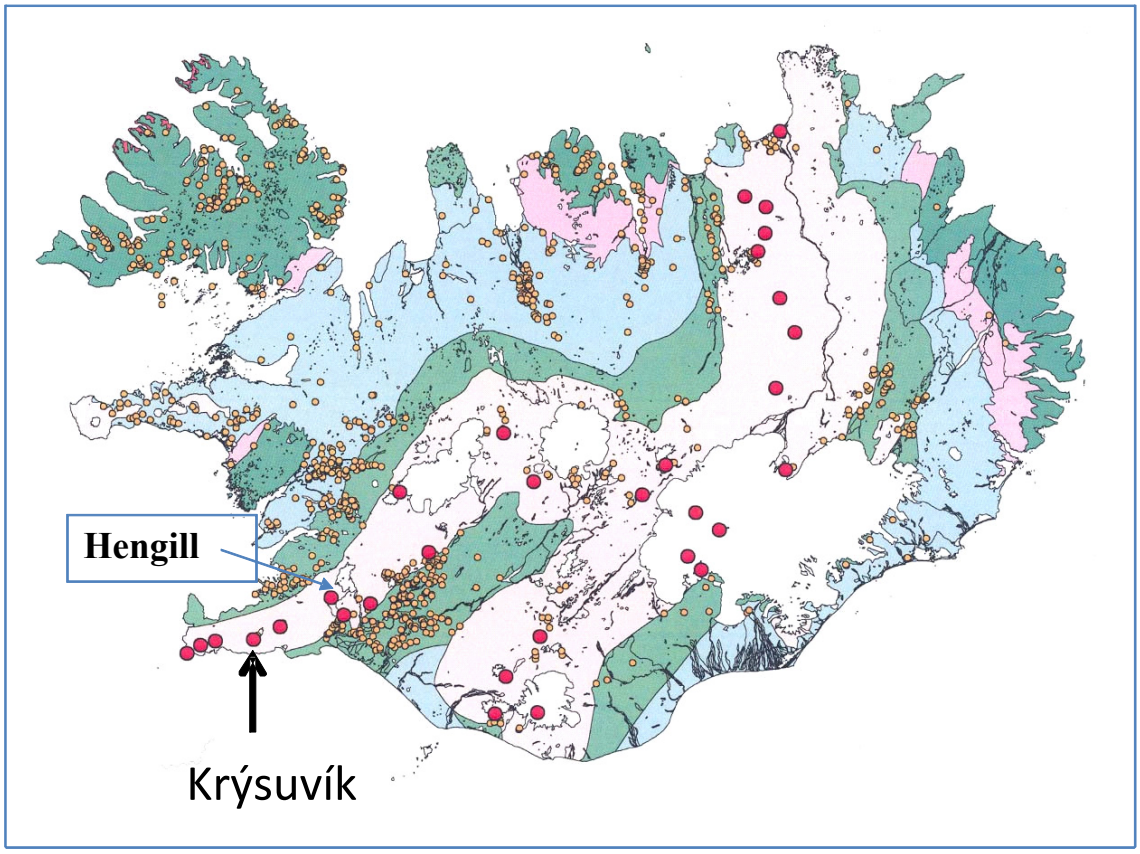

FIGURE 11: A simplified geological and geothermal map of Iceland; light pinkish gray is late Quaternary rocks; light green is rocks of Plio-Pleistocene age (0.8-3 My); light blue is Tertiary 3-8 My; pink is Tertiary (8-10) My; and dark green is Tertiary > 10 My; large red dots are high-temperature geothermal areas and yellow dots are low-temperature areas

Two major hyaloclastite ridges trending NE-SW dominate the Krýsuvík area. Faulting in the area is also mainly NE-SW. The rocks are of basaltic origin and from different periods, some of it being erupted under glaciers. The different geological formations are either hyaloclastite erupted during the last few glacial periods, or basaltic lavas with plagioclase or porphyritic lavas erupted during the last few interglacial periods. Kamah (1996) describes the geology of the Krýsuvík area. The rocks are basaltic and occur as olivine tholeiites, usually fine grained to medium grained. Dolerites made of coarse-grained basalt intrude into the interglacial basalt; glassy basalts are referred to as pillow lava. There are craters in several places. The stratigraphy within well KR-02 shows alternating series of hyaloclastite and basaltic lavas intruded by dykes.

Also found in the Krýsuvík area are historical lava flows (erupted after AD 870) that usually emanate from the volcanic fissure swarm trending NE–SW (N45ºE). The dykes in the area also have a NE–SW trending direction. Geothermal manifestations are located near the main structures and often have a NE–SW trending direction.

Surface hydrothermal alteration is probably mainly caused by shallow intrusive bodies, such as dykes, and major geostructures / faults. In each area, the alteration grade varies slightly from the peripherals to the centre of the geothermal manifestations. In the high-grade alteration zone, the temperature of the water at the surface and in soils varies from 80 to 93˚C. The alteration minerals are mainly clay and mixed-clay minerals, such as: kaolin, smectite, silica, calcite, iron oxides, zeolite and chlorite. Well KR-02 is 1,200 m deep and its maximum temperature is 350°C.

The Schlumberger sounding method has been used to explore the geothermal areas on the outer Reykjanes Peninsula in the 1970s and 1980s. The resistivity measurements revealed the existence of a zone of low resistivity, below 6 Ωm, along the plate boundary, associated with high temperatures. The resistivity values in the subsurface vary with temperature. Outside the low-resistivity zone, the resistivity is about 10-12 Ωm (Georgsson, 1984).

5.2 Processing TEM and MT data from the Krýsuvík geothermal area

The resistivity structure of the Krýsuvík geothermal field was analysed using MT and TEM data (Hersir et al., 2009). Electrical resistivity data were analysed from 12 sites along profile KRY6, shown in Figure 12. The profile lies almost perpendicular to the geological structures that trend in the NE-SW direction. The data are composed of two data sets, TEM soundings and MT soundings. The TEM data were acquired with equipment from Geonics in Canada, using a transmission coil of 300 x 300 m and two receiver coils, a standard 3-D coil and a larger 5 x 5 m coil. The advantage of using the large coil is that it increases the depth of investigation, which depends on the effective area of the

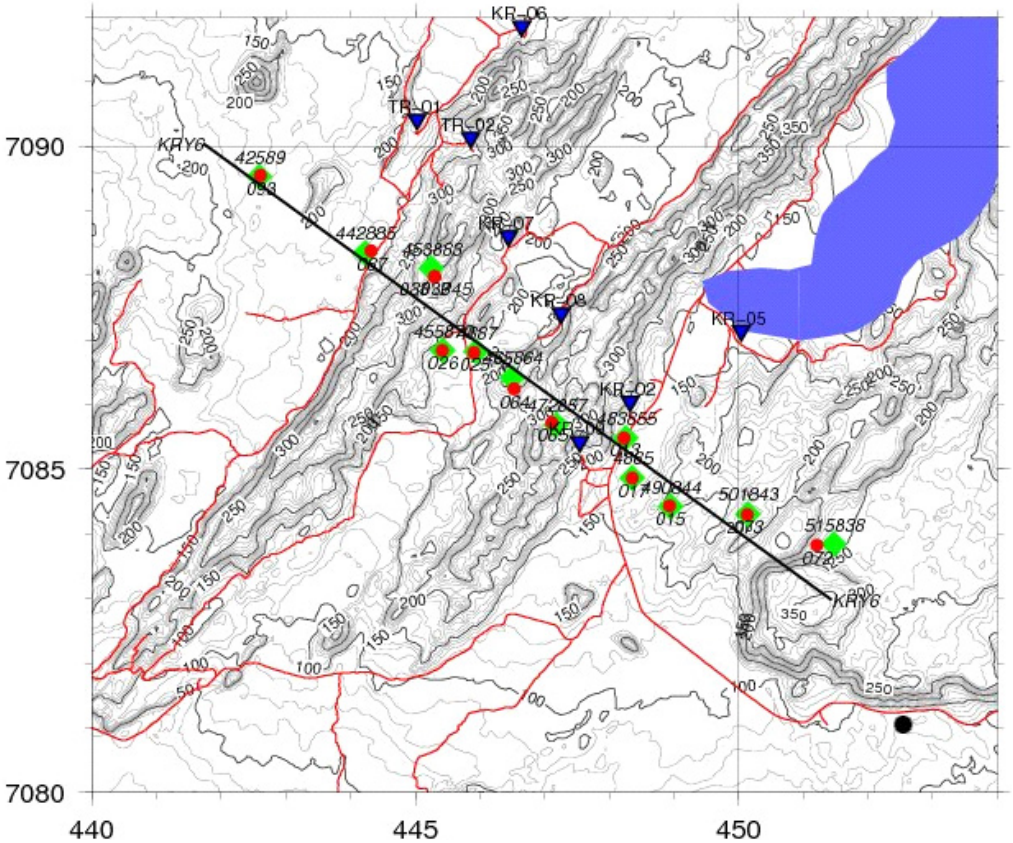

FIGURE 12: Location of TEM (gray/green diamonds) and MT (red/dark dots) sites, profile KRY6 and drillholes (blue/dark triangles) in the Krýsuvík area

receiver coil. Two frequencies were used: a high frequency 25 Hz with data collected through the standard coil (3-D mode) and 2.5 Hz using both the standard coil and the larger coil. Data were stacked and processed using the TEMX software that runs on a computer with a LINUX operating system. TEMX processing involves editing or removing noise filled data to expose the true signals.

After processing, the data points were plotted as a smooth curve on a bilogarithmic scale and modelled using the TEMTD program (forward or Occam inversion). The TEMTD program generates and estimates automatically the characteristics of the misfit curve, compared to the measured data. A few sites were modelled using the forward approach. The fits were assumed reasonable at χ^2 (Chsq) less than 1. Results of the inversion of the TEM soundings are presented in Appendix I.

The magnetotelluric (MT) data were acquired using MT-U5A magnetotelluric instruments made by Phoenix in Canada. The instruments, an A/D logger, magnetometer coils and an electric dipole, were calibrated before and after the survey programme in the field. Four sets of instruments (1857, 1926, 1925 and 1924) were deployed in the field. MT instrument 1925 was used as a remote reference station throughout the surveying period, located far away from the survey area. Its average distance from each measuring station was around 25 km. The remaining three instruments were running simultaneously with the remote reference station. Three sets of instruments (1924, 1925 and 1926) measured 5 components (H_x, H_y, H_z, E_x and E_y), while instrument 1857 measured only the two electrical components, namely E_x and E_y. Since the magnetic field tends to be stable in the same area, the impedances, based on data from instruments 1857, were computed using magnetic fields H_x and H_y from a nearby station that ran simultaneously.

The MT raw data were processed using the SSMT2000 program from Phoenix that transforms the data from the time domain to the frequency domain. The input data included the calibration data, the remote reference data and the local data from the roving instruments. The input data was reviewed for time consistency between the remote station and the field instruments, time series correlations of MT components, edited information at each site, computing Fourier coefficients and processing the data from the time domain to the frequency domain. The MT signals were edited based on the remote reference to reduce or minimise upward and downward bias effects caused by the electric and magnetic fields, respectively. The impedances were computed from the electrical and magnetic field spectra whereas the noise was minimised by auto and cross power spectral analysis, using the remote reference. The computed frequency data were edited using the MT-editor program from Phoenix to remove bad data points and produce as smooth a curve as possible (see Figure 8). The data were saved as MPK and EDI files for further modelling stages. The results for each MT station are shown in Appendix II. Finally, data sets from the TEM and MT were jointly inverted using the TEMTD program. The results are given in Appendix III. The procedure is summarised in the diagram shown in Figure 13.

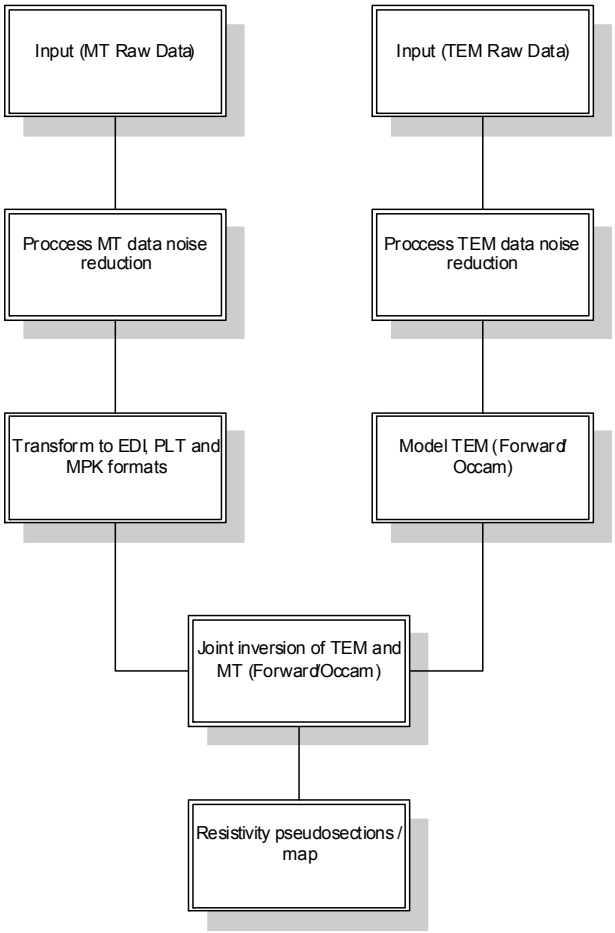

FIGURE 13: Flow chart diagram for the TEMTD inversion procedures

5.3 The resistivity structure of the Krýsuvík high-temperature geothermal field

The location of the low-resistivity structures is related to the hyaloclastite ridges, the two major geological structures in the area, which both trend in a NE-SW direction. The results of the inversion of the TEM stations only is shown in Figure 14 while the model for the joint inversion of TEM and MT is shown in Figures 15-17, with the difference in the presentation down to increasing depth levels, 3, 5 and 10 km below sea level. The lithological succession (stratigraphy) from borehole KR-02 was integrated into the interpretation of the layers. The dominant hydrothermal alteration minerals that relate to the resistivity structure of the area are shown in Figure 18. The hydrothermal alteration minerals considered are smectite, zeolite, chlorite, epidote, and mixed-clay minerals.

5.3.1 The resistivity profile KRY-6, using only the TEM data

The resistivity profile KRY-6, based only on the results of the TEM measurement, is shown in Figure 14. The TEM measurements reveal the resistivity structure in the Krýsuvík geothermal system to a maximum depth of approx. 1,000 m. In the central part of the cross-section, a conductive zone is seen that probably defines the status of alteration, or possibly high permeability caused by faults, shearing or fracturing associated with fluid circulation in the region. High resistivity on the surface and in near-surface rocks relates to unaltered volcanic rocks (basalts, lava flows and hyaloclastites). The lateral extension of the conductive structure is much larger at deeper levels than close to the surface. The conductive structure is assumed to be caused by altered clay minerals and the presence of water in pores in the hyaloclastite rocks. The conductive zone shows a conical shape, probably reflecting the effect of the upflow of geothermal fluid in the system.

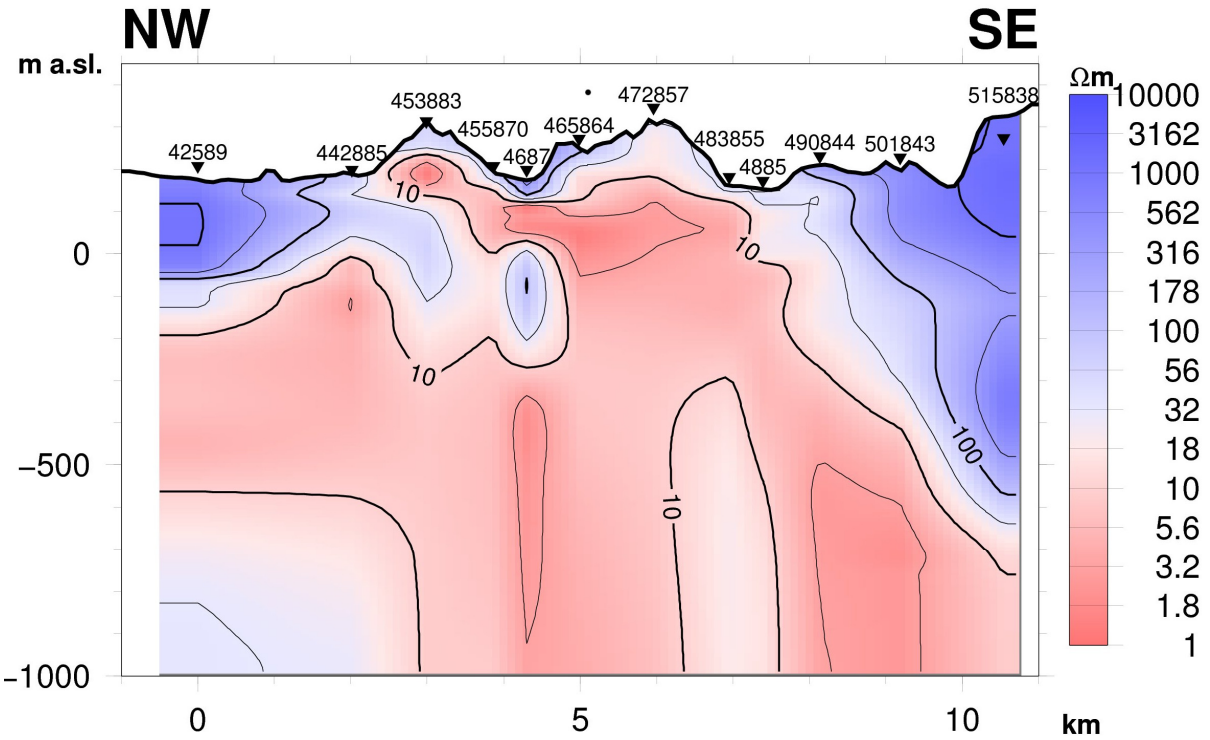

FIGURE 14: Krýsuvík resistivity profile KRY-6 using only the TEM data

5.3.2 The resistivity profile KRY-6 using the joint inversion of TEM and MT data

The joint inversion of the TEM and MT data probes deeper into the subsurface than by using only TEM data. The results based on the use of the TEMTD program show the resistivity structure from the surface to depths of several kilometres. To visualize the structures more clearly, the results are presented using three different maximum depths. The selected depths are 3 km as presented in Figure

15, 5 km as in Figure 16 and 10 km as in Figure 17. As mentioned above, the rocks near the surface are resistive reflecting fresh rocks (unaltered ones). The conductive cap below the surface layer extends to a depth of about 750 m in the central part, but down to 1,500 m at the flanks of the profile. Below that, higher resistivities are found, related to resistive high-temperature alteration, or possibly intrusive bodies, regarded herein as the resistive core, extending to a depth of more than 10 km. However, two conductive structures are seen crossing the resistive core to deeper levels, possibly associated with some permeable main structures.

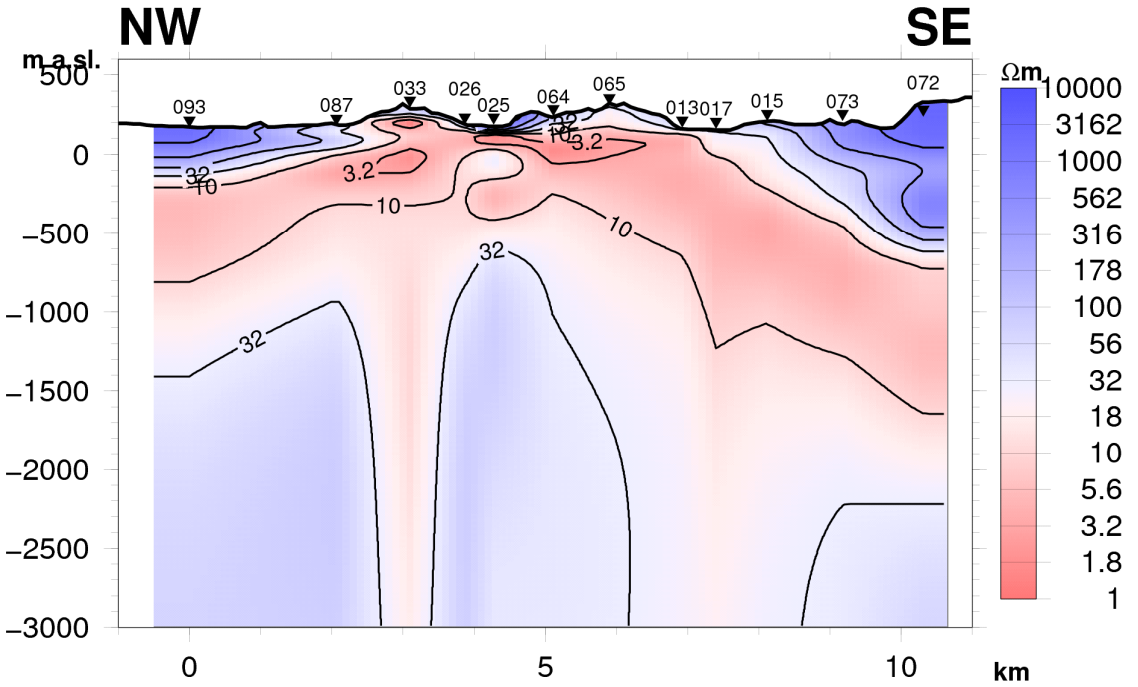

FIGURE 15: Interpretation of the Krýsuvík resistivity profile KRY-6 using TEMTD down to a maximum depth of 3,000 m

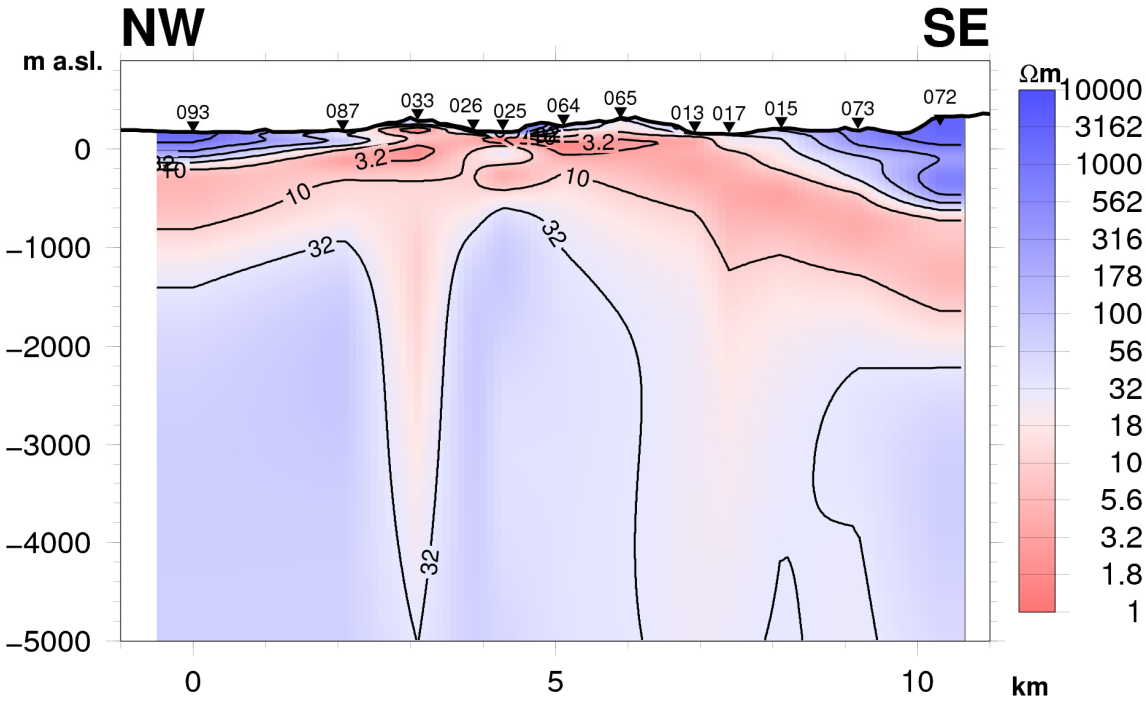

FIGURE 16: Interpretation of the Krýsuvík resistivity profile KRY-6 using TEMTD down to a maximum depth of 5,000 m

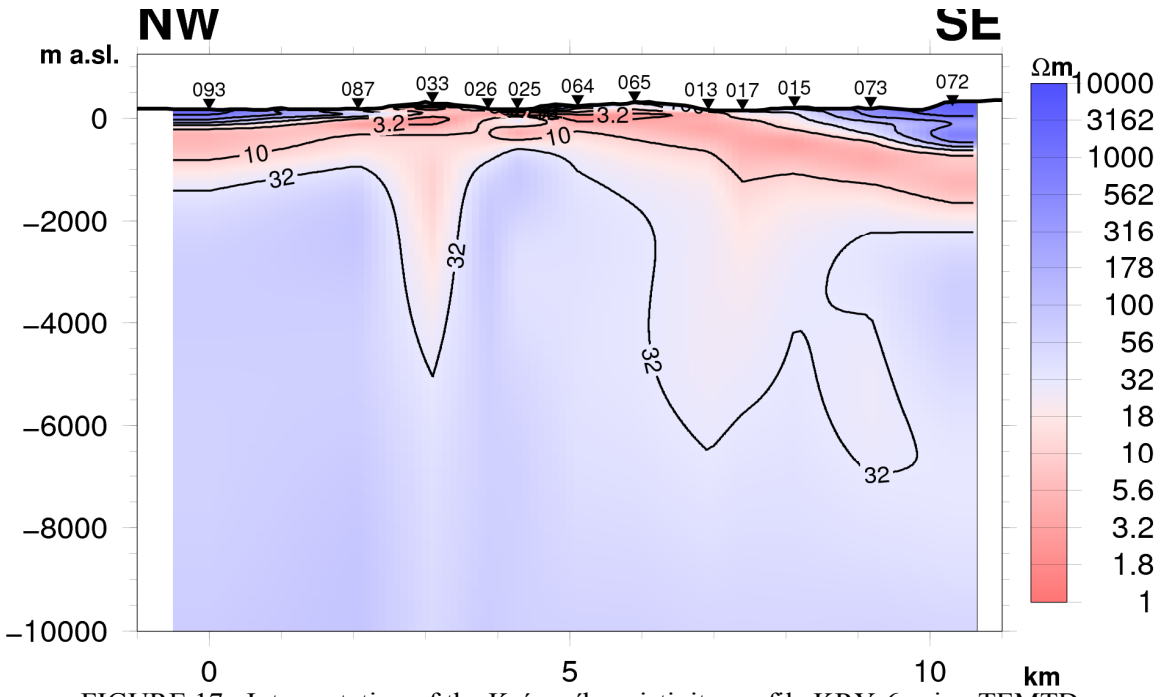

FIGURE 17: Interpretation of the Krýsuvík resistivity profile KRY-6 using TEMTD down to a maximum depth of 10,000 m

5.3.3 Hydrothermal alteration minerals

Figure 18 shows the integration of data from borehole KR-02 into the resistivity profile based on the inversion of the TEM data (Figure 14). Minerals analysed from borehole KR-02 include calcite, phillilosite, stibnite, heulandites, laumontite, wairakite, prehnite, albite, epidote, sphene, gypsum, limonite, pyrite, smectite, mixed clay minerals, swelling chlorite and chlorite. The minerals represent secondary alteration of the basaltic rocks. The primary minerals in basaltic rocks, however, are olivine, pyroxene, Ca-rich plagioclase series (anorthite, bytownite and labdarite) and opaque (magnetite, haematite and ilminite) minerals. The interaction of hydrothermal fluids and primary minerals at various temperatures and pressures results in alteration of primary minerals to clay minerals and occurs in particular assemblages.

The relationship between resistivity and mineral alteration at different depths relates to the temperature status of the rocks, if not at present than at least in the past. Among the analysed minerals are smectite, mixed clays, zeolite, epidote and chlorite. At the top of the well, the temperature is about 100°C, with the low temperatures leading to the rocks becoming richer in smectite and zeolites, reflected through low resistivity. The smectite-zeolite zone extends from surface to about 150 m depth. The second zone consists of mixed-layer clays extending from 150 to about 400 m. The mixed-layer clays are more or less equally electrically conductive as the smectite and zeolites. The temperatures in this layer are between 150 and 220°C. The chlorite zone is located below the mixed-layer clays, and is more resistive. The chlorite zone extends from 400 to 750 m and the temperature in the chlorite zone is expected to be above 200°C. The resistive epidote-chlorite zone is located at a depth of 750 to 1,200 m but probably extends to much greater depths. This alteration represents high temperature, at least above 250°C.

A good correlation was found between the subsurface resistivity and hydrothermal alteration in the drillhole, as shown in Figure 18 and discussed earlier in this report. The dominant smectite-zeolite zone is found where the subsurface resistivity is relatively low (low-resistivity cap) while the resistive core correlates with the dominant deep alteration zone consisting of chlorite-epidote.

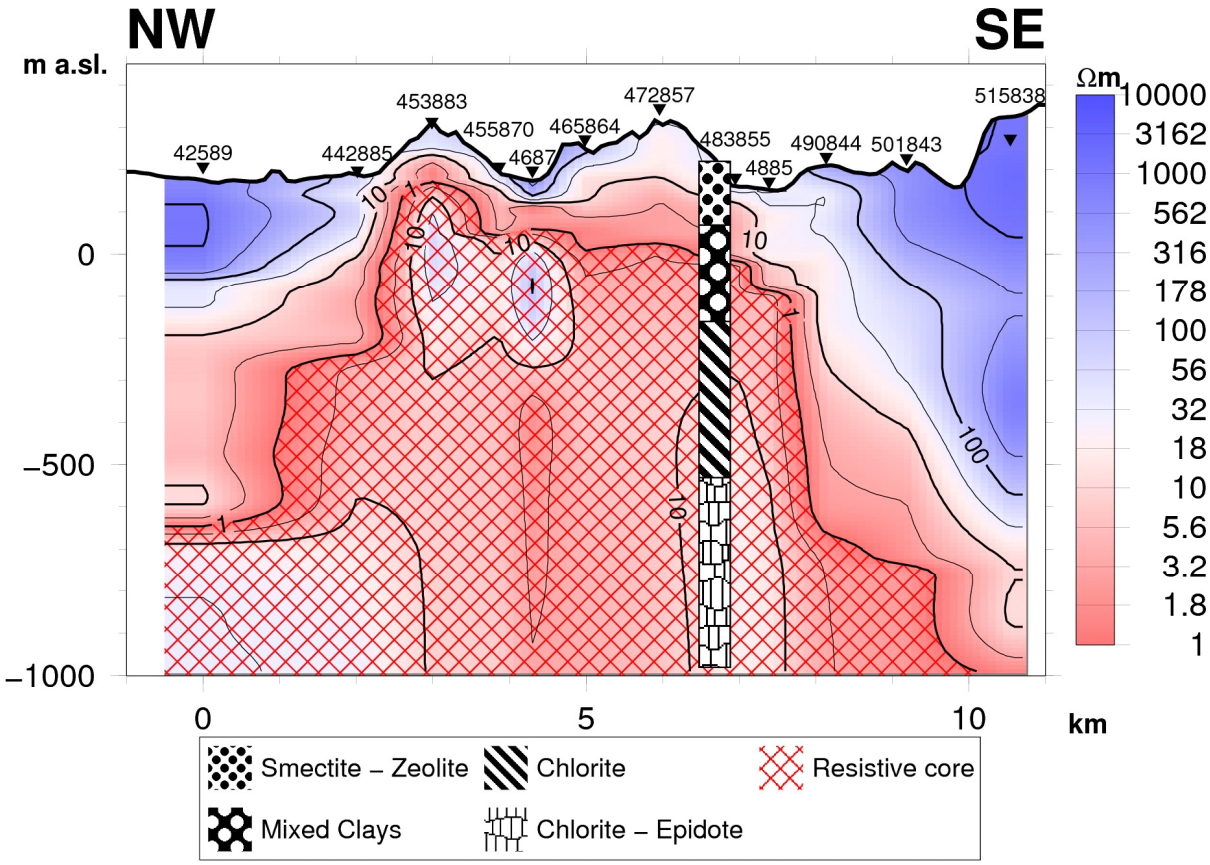

FIGURE 18: The Krýsuvík resistivity profile KRY-6 and hydrothermal alteration in well KR-2

6. CONCLUSIONS AND DISCUSSION

The study made here includes use of the TEM and MT electrical resistivity methods, data processing and finally jointly inverting the data. The soundings made are located on one profile, KRY-6, which is perpendicular to the main structural trend, which is NE-SW. In the resistivity profile, low resistivity associated with the smectite-zeolite alteration zone dominates the upper part where the temperature is also relatively low. The intermediate zone below relates to the mixed-layer clays, which are also conductive. In the resistive core below, epidote-chlorite alteration dominates, indicating higher temperatures, in excess of 250°C. This means that the conductive layer is mainly a clay cap, formed by secondary mineral alteration of smectite-zeolite type (Figure 18). The heat source of the geothermal water is probably related to intrusive bodies, located at deep levels.

The layering of hyaloclastite, the position and direction of the major structures, the high-temperature geothermal manifestations and the resistivity structure seen in profile KRY-6, can contribute to a model of the geothermal system of the area. Tectonic faulting is mainly through downthrow eastwards across the profile, from the west to the eastern part in the area. In the central part, a shallow subsidizing basin (graben) exists. The model defines an extensional faulting system with dyke intrusions. The intrusion of dykes occurs mainly along the main fault system. The dyke swarm may extend several kilometres along the fault system.

The resistivity profile shown in Figures 14-18 indicates two major conductive zones crossing the high-resistivity core to about 6 km depth. At the surface, these two structures may connect with the major fault systems observed there. It is possible that these structures are responsible for main fluid

transport, and for recharging and discharging geothermal fluids from the heat source. The drilling programme should aim at a depth ranging from 1,200 to at least 1,500 m, focusing on these two main structures.

ACKNOWLEDGEMENTS

I would like to extend my sincere appreciation to everyone who helped in the production of this report. However, it is difficult to acknowledge each and every person who participated directly or indirectly. Therefore, I will mention only a few of them. First, I extend my sincere appreciation to the UNU-GTP organization for awarding me the scholarship to pursue the course in geothermal training in Iceland. I extend my appreciation to all the administrative team and technical co-workers for their hard work during the study. To mention just a few of them: Dr. Ingvar Birgir Fridleifsson, Mr. Lúdvík S. Georgsson, Mrs. Thórhildur Ísberg and Mr. Markús A.G. Wilde for their daily participation and responsibilities during the course and the study.

I wish to acknowledge my supervisor, Mr. Gylfi Páll Hersir, for his keen follow-up of the study, tireless reading, correcting the report and daily advice during the study time. I extend my sincere acknowledgement to the ÍSOR administration team and their personnel for assistance in various lectures and material support. To mention a few: Mr. Arnar Már Vilhjálmsson, Mr. Knútur Árnason and Mr. Hjálmar Eysteinsson. The aforementioned personnel greatly contributed to the understanding of the study.

I would like to acknowledge the Government of Tanzania, through the Ministry of Energy and Minerals, Geological Survey of Tanzania to accept my request to attend the six months programme in Iceland and my exemption from my daily duties. In this particular case, I would like to acknowledge Prof. A.H. Mruma, the Chief Executive of Geological Survey of Tanzania (GST) on behalf of the rest.

I extend my appreciation to ICS-UNIDO in Italy and the Trieste University in Italy for their initial efforts in drawing my interest towards geothermal development. As a student at Trieste University and supported by ICS-UNIDO, I would like to extend my appreciation to Mr. Pipan Michelle from the University of Trieste and Mr. Ghribi Mounir on behalf of the Director of ICS-UNIDO, as well, for their devotion to the support and development of geothermal energy.

Last, but not the least, I would like to thank my fellow students in the course for their good cooperation during the study.

REFERENCES

Árnason, K., 1989: *Central loop transient electromagnetic sounding over a horizontally layered earth*. Orkustofnun, Reykjavík, report OS-89032/JHD-06, 129 pp.

Árnason, K., 2006. *TEMTD, a programme for 1D inversion of central-loop TEM and MT data.* Short manual. ISOR – Iceland GeoSurvey, Reykjavík, internal report (in English), 17 pp.

Árnason, K., Flóvenz, Ó., Georgsson, L.S., and Hersir, G.P., 1987a: Resistivity structure of high-temperature geothermal systems in Iceland. *International Union of Geodesy and Geophysics (IUGG) XIX General Assembly*, *Vancouver Canada, Abstracts V*, 477.

Árnason, K., Haraldsson, G.I., Johnsen, G.V., Thorbergsson, G., Hersir, G.P., Saemundsson, K., Georgsson, L.S., Rögnvaldsson, S.Th., and Snorrason, S.P., 1987b: *Nesjavellir-Ölkelduháls, surface exploration 1986.* Orkustofnun, report OS-87018/JHD-02 (in Icelandic), 112 pp+maps.

Árnason, K., Karlsdóttir, R., Eysteinsson, H., Flóvenz, Ó.G., and Gudlaugsson, S.Th., 2000: The resistivity structure of high-temperature geothermal systems in Iceland. *Proceedings of the World Geothermal Congress 2000*, *Kyushu-Tohoku, Japan,* 923-928.

Berdichevsky M.N., 1999: Marginal notes on magnetotellurics. *Surveys in Geophysics, 20*, 341-375.

Cagniard, L., 1953: Basic theory of magneto-telluric method of geophysical prospecting. *Geophysics*, *18,* 605-635.

Chiragwile, S. A., 2007: *Petrophysical properties of Kahama granitoids and their significance in the interpretations of aerogeophysical anomalies.* University of Dar es Salaam, MSc thesis, 129 pp.

Clifton, A., Pagli, C., Jónsdóttir, J., Eythórsdóttir, K. and Vogfjörd, K., 2003: Surface effects of triggered fault slip on Reykjanes Peninsula, SW Iceland. *Tectonophysics, 369*, 145-154.

Dakhnov, V.N., 1962: Geophysical well logging. *Q. Colorado Sch. Mines, 57-2*, 445 pp.

Flóvenz, Ó.G., Spangenberg, E., Kulenkampff, J., Árnason, K., Karlsdóttir, R., and Huenges, E., 2005: The role of electrical interface conduction in geothermal exploration. *Proceedings of the World Geothermal Congress 2005, Antalya Turkey*, CD, 9 pp.

Georgsson, L.S., 1984: Resistivity and temperature distribution of the outer Reykjanes Peninsula, Southwest Iceland. *54th Annual International SEG Meeting, Atlanta, Expanded Abstracts*, 81-84.

Gubbins, D., 2004: *Time series analysis and inverse theory for geophysicists*. Cambridge University, 282 pp.

Henn, F., Durand, C., Cerepi, A., Brosse, E., and Giuntini, A., 2007: DC conductivity, cationic exchange capacity, and specific surface area related to chemical composition of pore lining chlorites. *Colloid and Interface Science*, *311*, 571–578.

Hermance, J.F., 1973: Processing of magnetotelluric data. *Earth and Planetary Interiors*, *7*, 349 - 364, Netherlands.

Hersir, G.P., and Björnsson, A., 1991: *Geophysical exploration for geothermal resources. Principles and applications.* UNU-GTP, Iceland, Report 15, 94 pp.

Hersir, G.P., Rosenkjær, G.K., Vilhjálmsson, A.M., Eysteinsson, H., and Karlsdóttir, R., 2009: *The Krýsuvík geothermal field. Resistivity soundings 2007 and 2008*. ÍSOR - Iceland GeoSurvey, Reykjavík, report (in Icelandic), in prep.

Jones, A.G., Chave, A.D., Egbert, G., Auld B., and Bahr, K., 1989: A comparison of techniques for magnetotelluric response function estimation. *J. Geophys. Res., 94(B10),* 14201-14213.

Kamah, M.Y., 1996: Borehole geology, hydrothermal alteration and temperature evolution of well KR-2, Krýsuvík, SW-Iceland. Report 5 in: *Geothermal Training in Iceland 1996,* UNU-GTP, Iceland, 71-102.

Poe, B.T., Romano, C., Varchi, V., Misiti, V., and Scarlato, P., 2008: Electrical conductivity of a phonotephrite from Mt. Vesuvius: The importance of chemical composition on the electrical conductivity of silicate melts. *Chemical Geology, 256*, 193–202.

Simpson, F., and Bahr, K., 2005: *Practical magnetotellurics*. Cambridge University Press, UK, 254 pp.

Smirnov, M., Korja, T., Dynesius, L., Pedersen, L.B., and Laukkanen E. 2008: Broadband magnetotelluric instruments for near-surface and lithospheric studies of electrical conductivity: A Fennoscandian pool of magnetotelluric instruments. *Geophysica*, *44 (1-2),* 31–44.

Spichak, V., and Manzella, A., 2009: Electromagnetic sounding of geothermal zones. *Applied Geophysics, 68*, 459–478.

Sternberg, K.B., Wasburne, J.C., and Pellerin, L., 1988: Correction for the static shift in magnetotellurics using transient electromagnetic soundings. *Geophysics, 53-11*, 1459-1468.

Stoldt J., 1981: *Algorithms for magnetotelluric calculations in the frequency domain*. Phoenix Geophysics, Denver, Canada, 104 pp.

Telford, W.M., Gedart, L.P., and Sheriff, R.E., 1990: *Applied Geophysics* (2nd ed.). Cambridge University Press, UK, 770 pp.

Tikhonov, A.N., 1950: Determination of the electrical characteristics of the deeper strata of the earth's crust. *Dokl. Akad. Nauk USSR, 7 -2.*

Vozoff, K., 1991: The magnetotelluric method. In: Nabighian, M.N (ed), *Electromagnetic methods in applied geophysics*, *2*, 641-711.

Wight, D.E., Bostick, F.X., and Smith, H.W., 1977: *Real time transformation of magnetotelluric data*. Electrical geophysical research laboratory, University of Texas, Austin, 93 pp.

Wright, H.M.N., Cashman K.V., Gottesfeld, E.H., and Roberts, J.J., 2009: Pore structure of volcanic crusts: Measurements of permeability and electrical conductivity. *Earth and Planetary Science Letters, 280,* 93-104.

Zhang, P., Roberts, R.G., and Pedersen, L.B., 1987: Magnetotelluric strike rules. *Geophysics*, *52*, 267-278.

Zhdanov, M.S., and Keller, G.V., 1994: *The geoelectrical methods in geophysical exploration*. Elsevier Scientific Publishing Co., 873 pp.

Zonge, K.L., and Hughes, L.J., 1991: Controlled source audio-frequency magnetotellurics. In: Nabighian, M.N (ed), *Electromagnetic methods in applied geophysics*, *2*, 713-810.

APPENDIX I: TEM 1-D inversion models

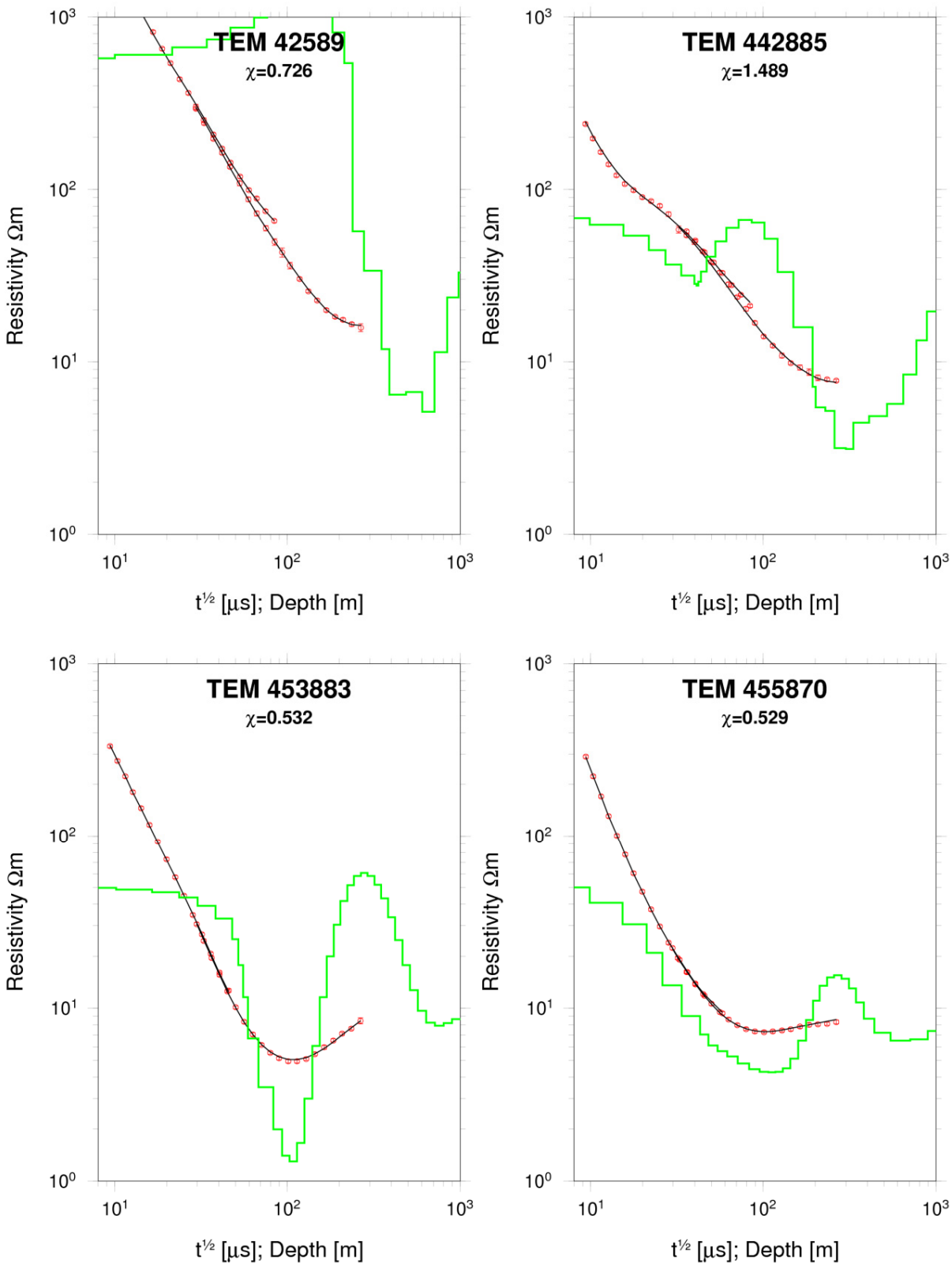

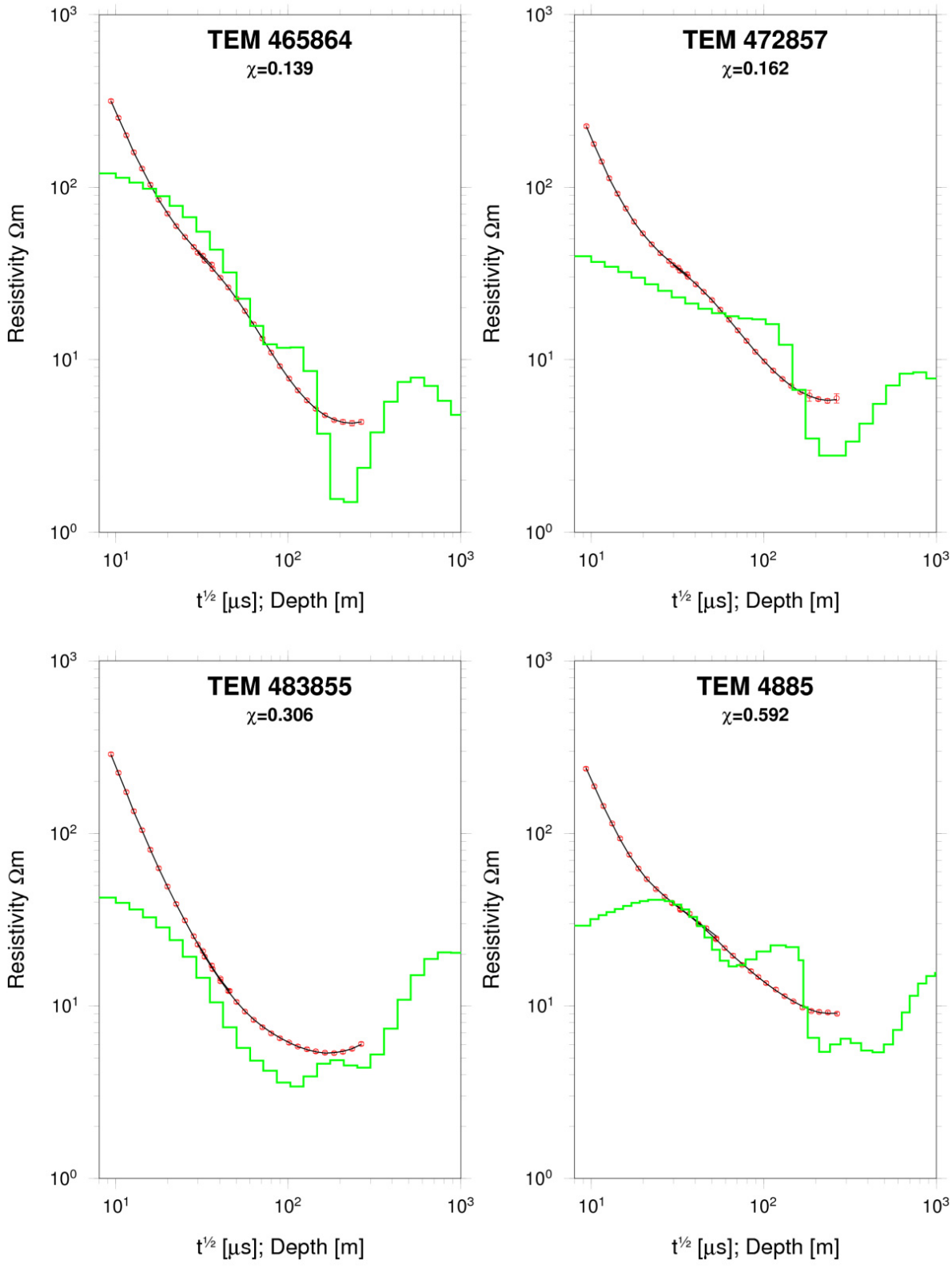
TEM 465864
χ=0.139
TEM 472857
χ=0.162
TEM 483855
χ=0.306
TEM 4885
χ=0.592
Resistivity Ωm
t½ [µs]; Depth [m]
10⁰
10¹
10²
10³

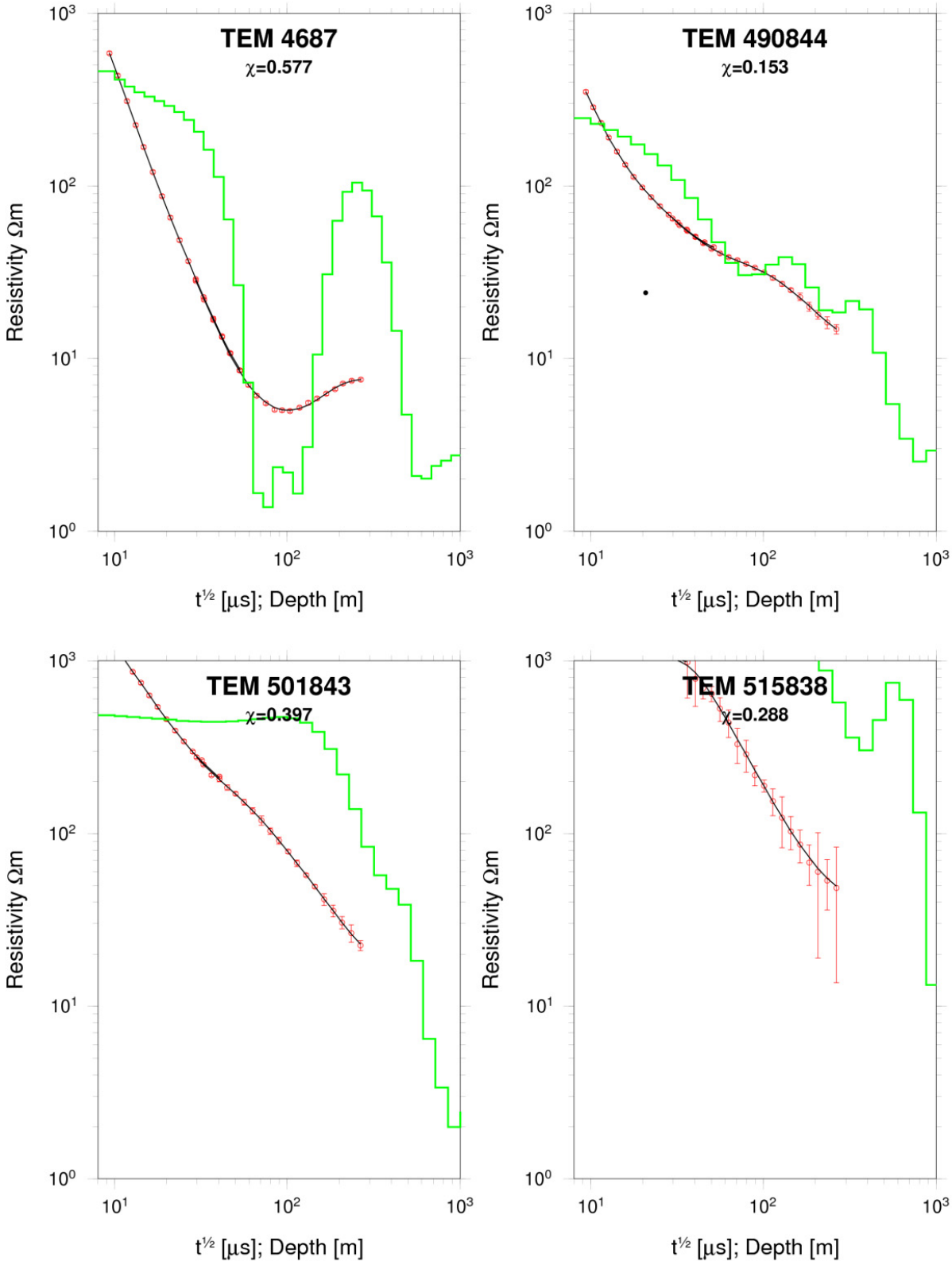
TEM 4687
χ=0.577
TEM 490844
χ=0.153
TEM 501843
χ=0.397
TEM 515838
χ=0.288
Resistivity Ωm
t½ [µs]; Depth [m]

APPENDIX II: MT data (EDI)

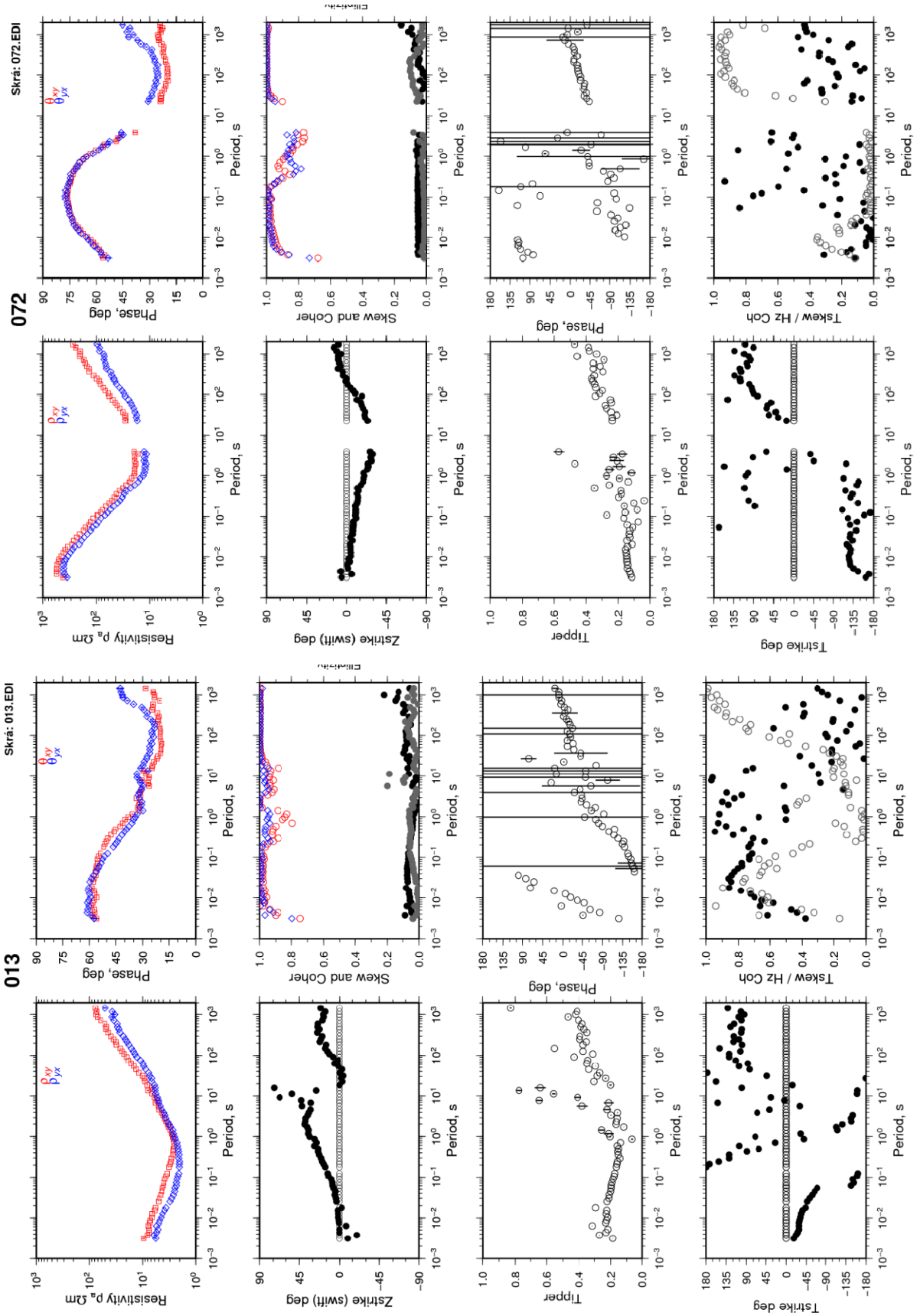

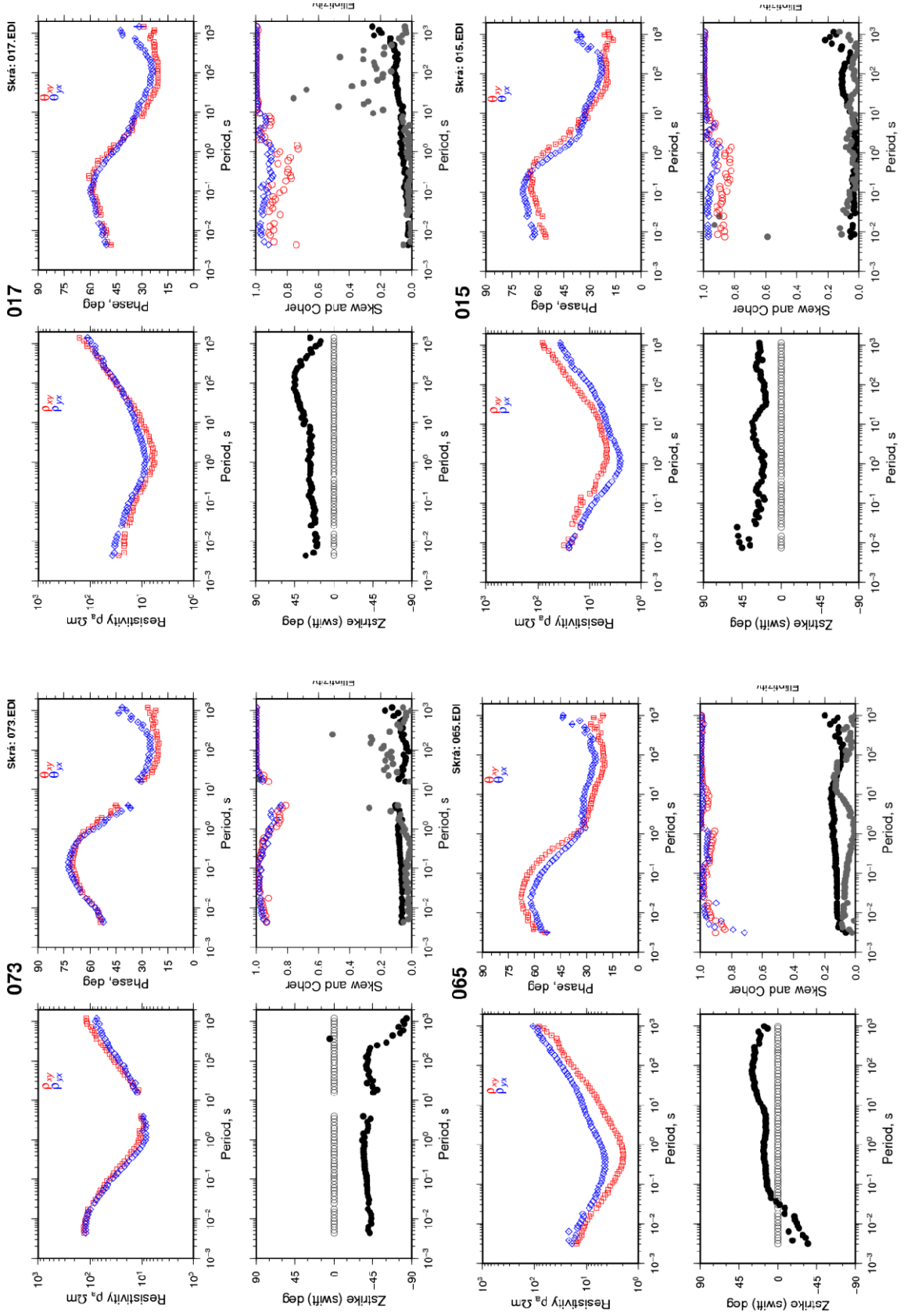
017
Skrá: 017.EDI
015
Skrá: 015.EDI
073
Skrá: 073.EDI
065
Skrá: 065.EDI
Resistivity ρa Ωm
Phase, deg
Skew and Cohер
Zstrike (swift) deg
Period, s
θxy
θyx
ρxy
ρyx

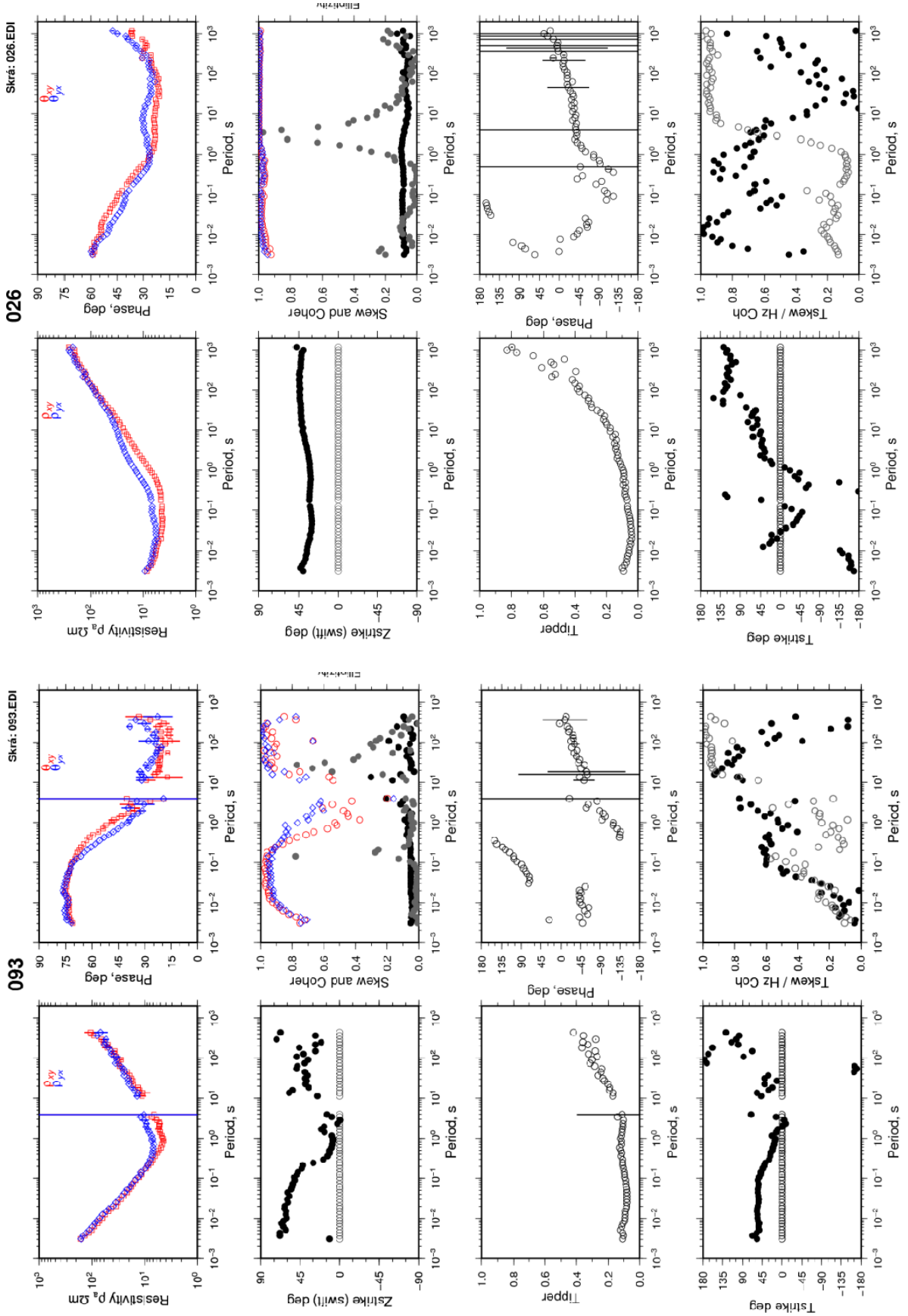
Skrá: 026.EDI
026
Skrá: 093.EDI
093
Resistivity ρa Ωm
Phase, deg
Zstrike (swift) deg
Skew and Coher
Ellipticity
Tipper
Phase, deg
Tskew / Hz Coh
Tstrike deg
Period, s

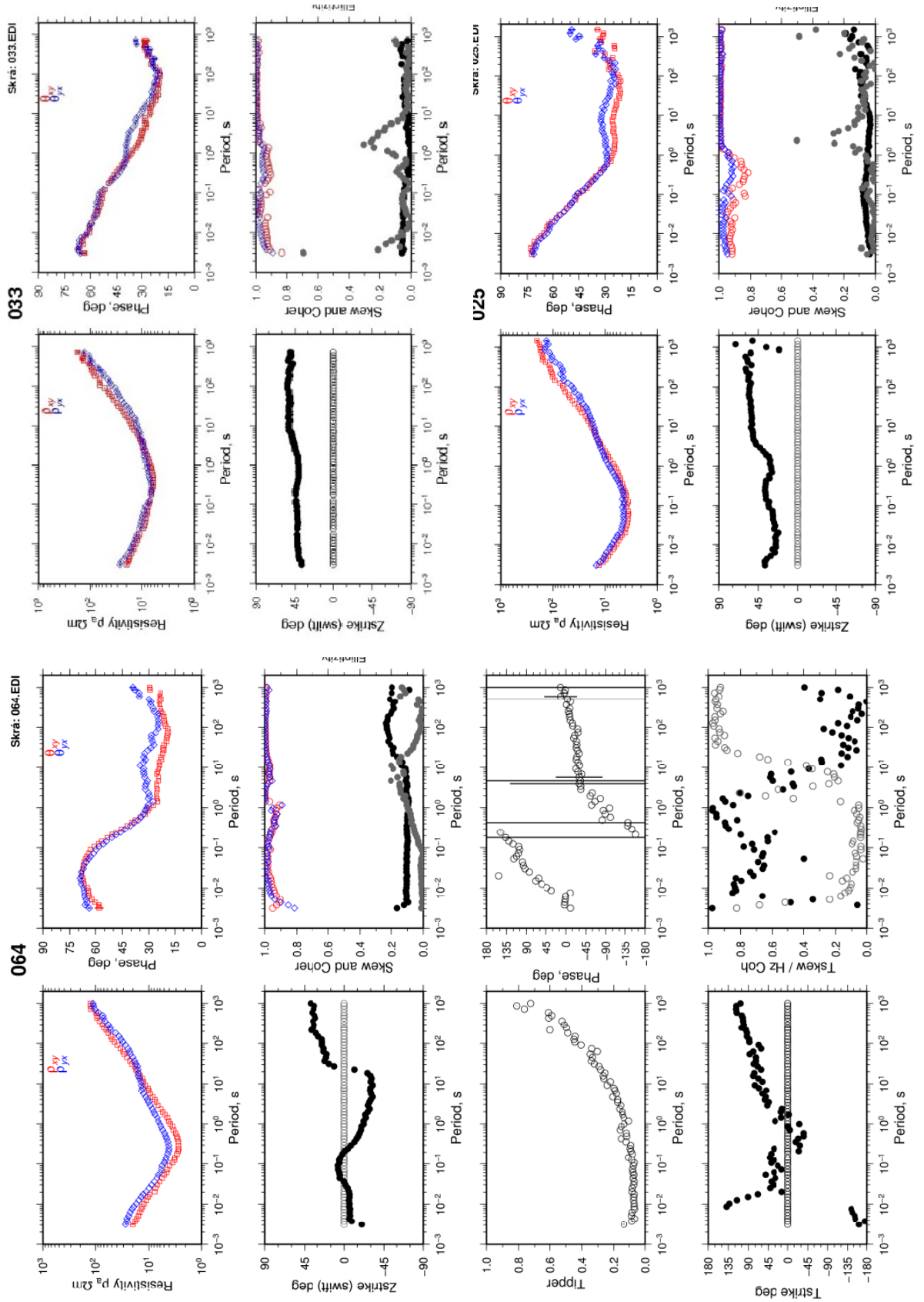
064
033
U25
Skrá: 064.EDI
Skrá: 033.EDI
Skrá: U25.EDI
Resistivity ρa Ωm
Phase, deg
Strike (swift) deg
Skew and Coher
Tskew / Hz Coh
Tstrike deg
Tipper
Ellipticity
Period, s
ρxy
ρyx
θxy
θyx

APPENDIX III: TEMTD 1-D TEM and MT inversion models

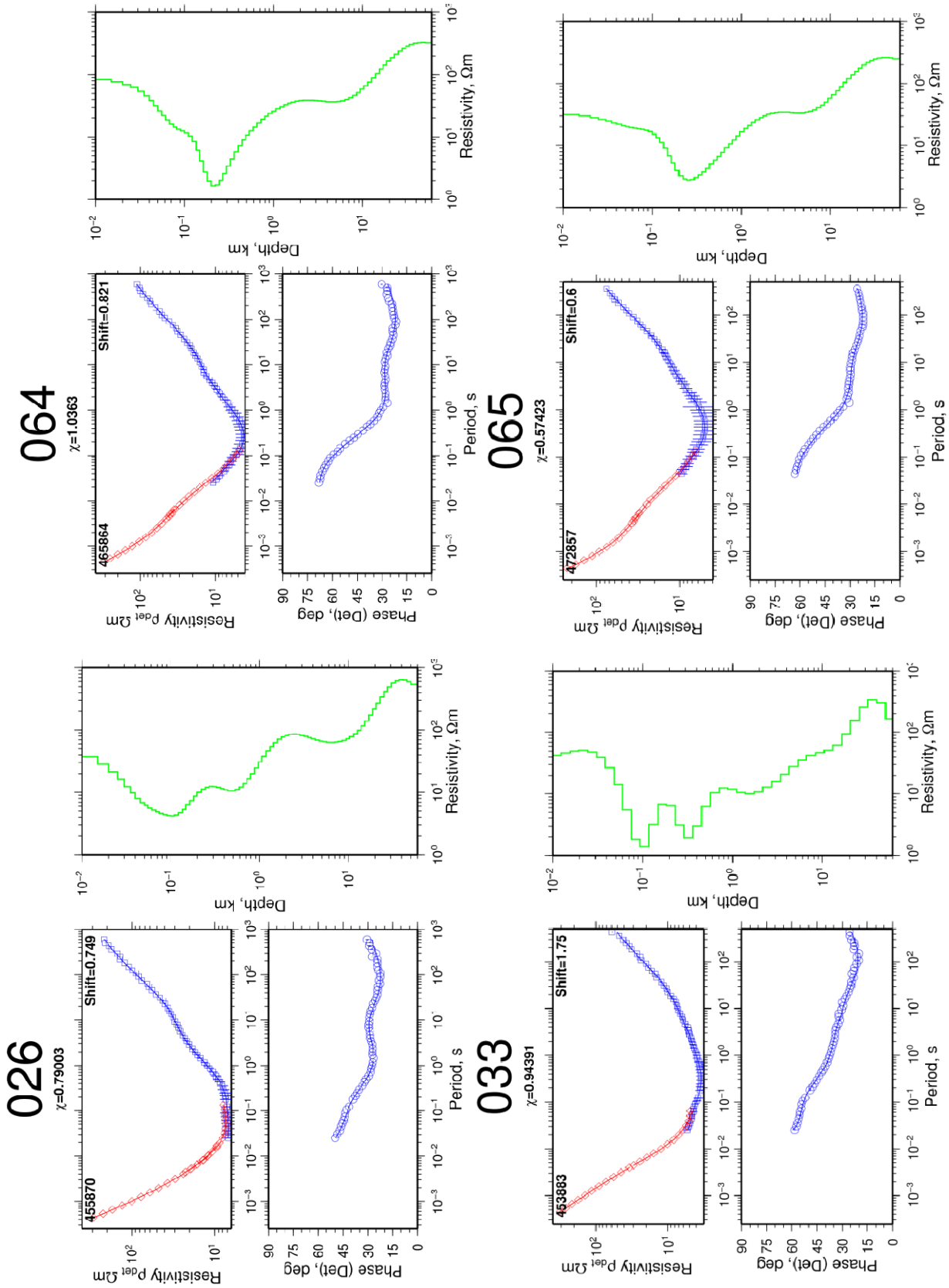

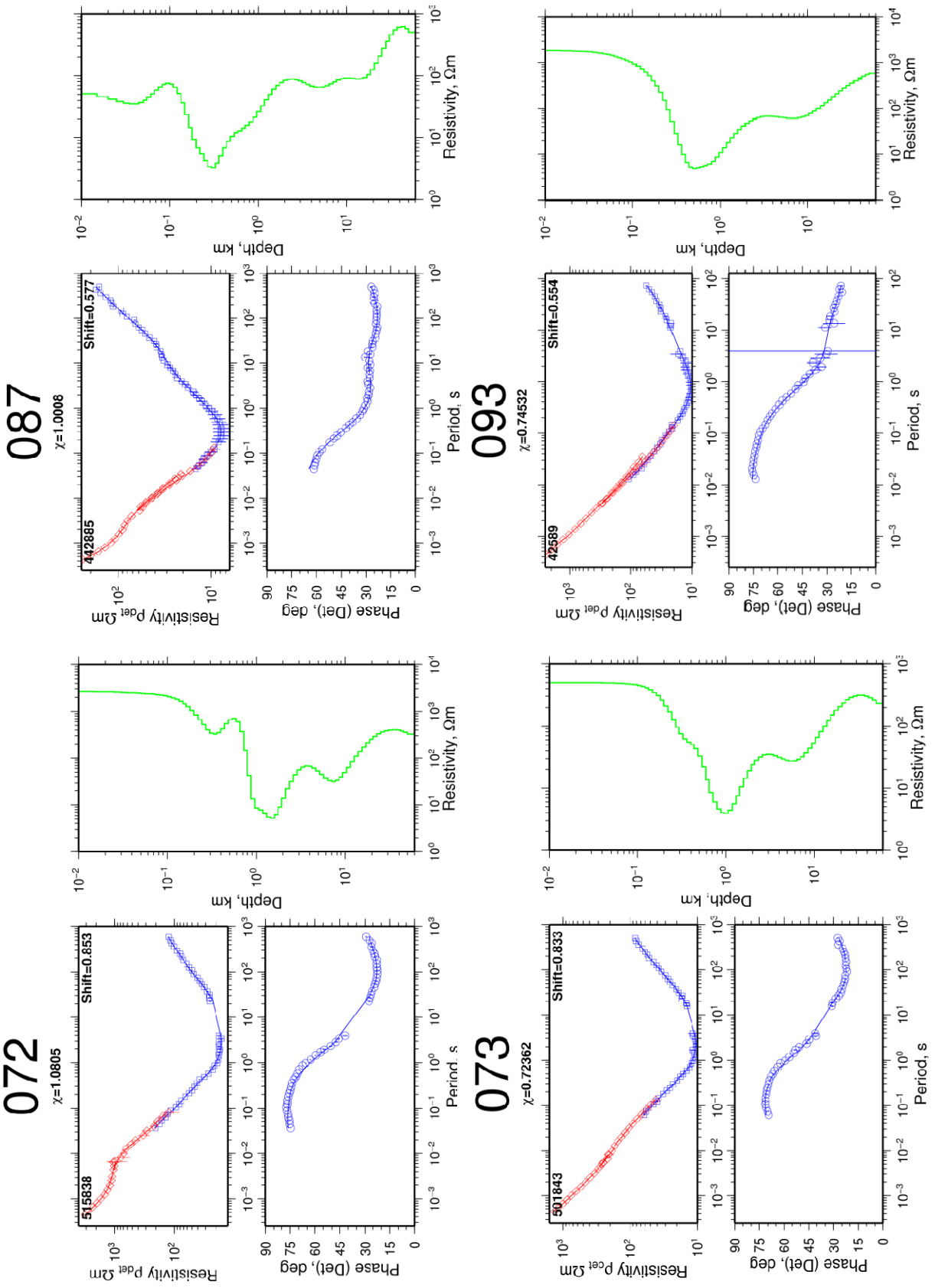
072
χ=1.0805
Shift=0.853
515838
Resistivity ρdet Ωm
Phase (Det), deg
Period, s
Depth, km
Resistivity, Ωm
087
χ=1.0008
Shift=0.577
442885
073
χ=0.72362
Shift=0.833
501843
093
χ=0.74532
Shift=0.554
42589